Understanding variability across the Crossroad transect from 3 years (2013 to 2015) of hydrographic data

By

Manare C. Sejeng

A thesis submitted in partial fulfilment for the
degree of Master of Science
in the

Faculty of Science
Department of Oceanography

Supervisors:
Prof. Isabelle Ansorge (UCT)
Dr. Tarron Lamont (DEA)
Dr. Christophe Maes (IRD)

October 2018

Declaration of Authorship

I, Manare Caroline Sejeng, declare that this thesis titled, ` Understanding variability across the Crossroad transect from 3 years (2013 to 2015) of hydrographic data' and the work presented in it are my own. I confirm that:

- This work was done wholly or mainly while in candidature for a research degree at this University.
- Where any part of this thesis has previously been submitted for a degree or any other qualification at this University or any other institution, this has been clearly stated.
- Where I have consulted the published work of others, this is always clearly attributed.
- Where I have quoted from the work of others, the source is always given. With the exception of such quotations, this thesis is entirely my own work.
- I have acknowledged all main sources of help.
- Where the thesis is based on work done by myself jointly with others, I have made clear exactly what was done by others and what I have contributed myself.

Signed: Signed by candidate
Date:

Abstract

The southwest continental shelf of Africa is characterized by a strong western boundary current with three interdependent components, namely the Agulhas Current, Agulhas Retroflection and Agulhas Return Current. This system plays a key role in setting oceanic conditions south of Africa. The Crossroad transect intersects both the Agulhas Current and Agulhas Return Current; a monitoring line established in 2013 to sample both the currents and determine inter-ocean fluxes, as well as the influence of the Agulhas Current on the Agulhas Bank shelf. The objective of the study was to examine both mesoscale and submesoscale features that influence the dynamic and variant nature of the Agulhas system. In this study we make use of Ship board Acoustic Doppler Current Profiler (SADCP), Conductivity Temperature and Depth (CTD), Thermosalinograph (TSG) and satellite Sea Surface Height data as main observations for analysis. The study also examines both the spatial and temporal characteristics of water properties across the Crossroad transect. The fundamental findings of the study include the abundance of both the mesoscale and submesoscale features observed in the Agulhas system, which are often overlooked. In addition, a noticeable variability in current measurements was observed, where velocity ranging from 2 to 2.5 m/s represented the Agulhas Current and 1.4 to 1.7 m/s, Agulhas Return Current. The position of the Agulhas Current and Agulhas Return Current displayed variation from 2013 to 2015, with the Agulhas Return Current exhibiting a meandering pattern in 2014 along the transect. Furthermore, an intrusion of cool (8 to 13 °C), lower salinity (34.8 to 35 psu) South Indian Central Water masses were also observed along the Agulhas Bank. The ability to combine altimetry and in situ data also contributed to the analysis of the results. Therefore, given the inherent advantage of satellite and in situ measurements, an overview of the variability across the Crossroad transect was determined.

Acknowledgements

“Trust in the Lord and lean not on your own understanding, in everything acknowledge God and He will direct your path” ~ Proverbs chapter 3 from verse 5 to 7. I am grateful for the immeasurable support from my family and friends who consistently encouraged me in this journey.

I take this opportunity to acknowledge as well my supervisors for their time and effort to assist in my academic development plan. Their passion and motivation towards the success and completion of this thesis has played an important role. The Crossroad transect cruise data was collected by Mr. Marcel van den Berg from Department of Environmental Affairs and for that I am truly grateful for providing the required datasets.

A special thanks goes to Dr. Marion Kersalé, Dr. Steven Herbette and everyone who contributed towards the success of the thesis.

Ke a leboga - Thank You

Dedication

I dedicate this thesis to my late grandmother Mrs. Mariam Ngoakoana Ramotlou

(koko Feke)

Robala ka khutso Monkani, Mmakgotse, Sibita.

And all my family members

List of Acronyms

AABW - Antarctic Bottom Water

AAIW - Antarctic Intermediate Water

AC - Agulhas Current

ACC - Antarctic Circumpolar Current

ARC - Agulhas Return Current

ADCP - Acoustic Doppler Current Profiler

AVISO - Arching, Validation and Interpretation of Satellite Oceanographic

CTD - Conductivity Temperature Depth

DUACS - Data Unification and Altimeter Combination System, or Developing Use of Altimetry for Climate Studies

GODAE - Global Ocean Data Assimilation Experiment

GHRSST - Group of High Resolution Sea Surface Temperature (GHRSST)

ITF - Indonesian Through-Flow

MADT-H - Maps of Absolute Dynamic Topography Heights

MSLA - Mean Sea Level Anomaly

MDT - Mean Dynamic Topography

MOC - Meridional Overturning Circulation

MZC - Mozambique Channel

NADW - North Atlantic Deep Waters

NASA - National Aeronautics and Space Administration

ROMS – Regional Ocean Model System

RSW - Red Sea Water

SDS- Scientific Data System

SEC - South Equatorial Current

SEMC - South East Madagascar Current

SICW - South Indian Central Water

SMOS - Soil Moisture and Ocean Salinity

SSALTO - Segment Sol multi-missions dALTimetrie, d'orbitographie et de localisation precise

SSH - Sea Surface Height

SSS – Sea Surface Salinity

SST - Sea Surface Temperature

STSW - SubTropical Surface Water

TSW - Tropical Surface Water

TSG- Thermosalinograph

List of Symbols

u - velocity component

v - velocity component

τ - time

λ - lamda

∂ - partial

ρ - density

p - pressure

Contents

LIST OF FIGURES

LIST OF TABLES

Chapter 1

Literature Review

1.1 An overview of salient features and dynamics of the Greater Agulhas Current system

Research focus has been directed towards an oceanic system constituting of surface, intermediate and deep ocean currents; the Atlantic Meridional Overturning Circulation (AMOC) (McPhaden and Zhang, 2002; Kuhlbrodt et al., 2007; Cunningham et al., 2007). The AMOC, according to Schiermeier (2007, 2013), stirs water from the top to bottom of the ocean. The overarching aim of this process is to transport warm water through the Atlantic towards the poles and cold water (salty enough to sink) flowing at great depths towards the tropics with current strength varying greatly as depicted in Figure 1.1.

Previous studies have shown that the AMOC has an important role in modulating climate variability through the coupling of the ocean and atmosphere. The AMOC's impact is evident in the redistribution of heat, salt, freshwater, nutrients and one of the natural and anthropogenic ocean sinks; carbon dioxide (CO_2) (Schmittner et al., 2007; Sabine et al., 2004). The formation of deep waters at high latitudes has also been identified as an important contributor towards driving ocean circulation carrying large concentrations of CO_2 to great depths, sequestering it from the atmosphere (Schiermeier, 2013). Through their impact on the AMOC and deep upwelling, changes in the Southern Ocean winds and buoyancy fluxes have the ability to regulate the ocean´s carbon storage capacity (Watson et al., 2005; Toggweiler et al., 2006). The amount of energy involved in the overall ocean circulation mechanism is substantial and quantified to about 2 000 trillion watts or 2 peta watts, which Schiermeier (2007) asserts to approximate 200 times the rate at which mankind uses energy, moreover the energy flow needed to drive the Earths climate.

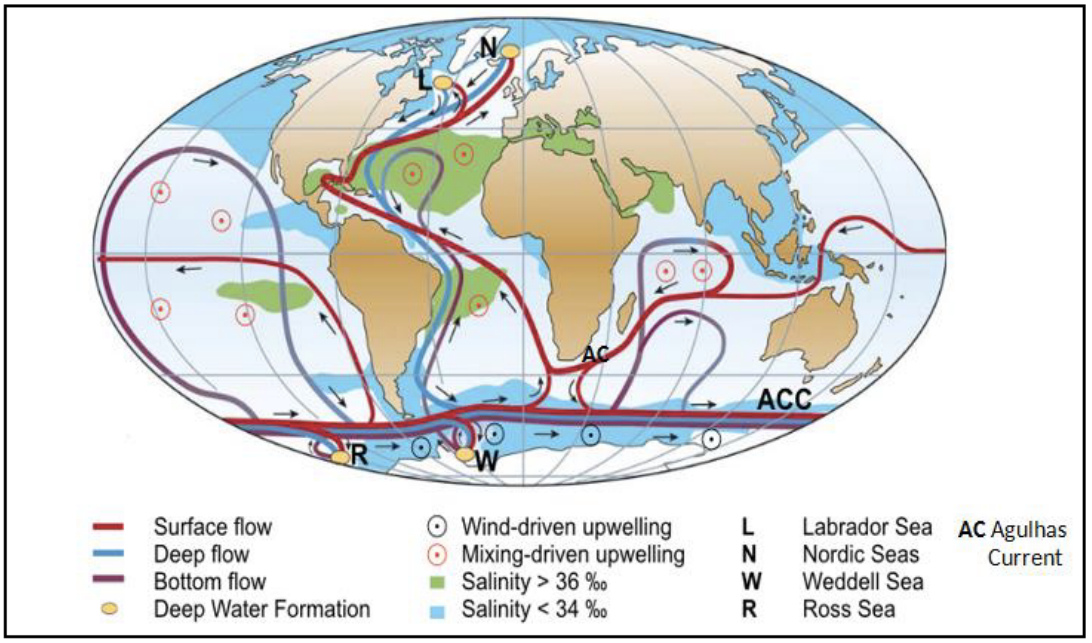

FIGURE 1.1: A simplified diagram of the AMOC representing surface and deep currents encompassing all ocean basins. Surface flows are indicated by red pathways while deep flows are indicated by blue pathways. Warm and saline waters flow northwards in the Atlantic Ocean. Wind driven upwelling is observed in the Southern Ocean. The modified diagram also indicates the Agulhas Current pathway. Adapted from (Kuhlbrodt et al., 2007).

The world´s major ocean basins are comprised of strong, persistent currents along western boundaries, which contribute towards driving the ocean circulation (Imawaki et al., 2013). Research documented by Imawaki et al., (2013) identified Western Boundary Currents (WBC) as the Gulf Stream, Brazil Current, Agulhas Current, Kuroshio and East Australian Current (EAC) with the foci being their role in basin scale circulation, regional variability and their influence on both oceanic and atmospheric processes. One of the most energetic systems across the globe is the Agulhas Current system, which plays a role in the marine environment along with its resources and ecosystems. The greater Agulhas Current system encompasses the following oceanographic features: The Agulhas Current and its sources, Agulhas Retroflection, Agulhas leakage and Agulhas Return Current as seen in Figure 1.2. Research based on the CMIP5 and EMIC ocean model outputs has shown that the AMOC is likely to weaken by approximately 11 to 34% (Morris et al., 2017). The Agulhas Current system acts to balance the AMOC through the Agulhas leakage as it feeds its upper limb through the exchange of water masses from the Indian Ocean to the Atlantic Ocean (Beal et al., 2011). The variations in the water mass exchange has been linked to the strength and position of the westerly winds (Morris et al., 2017). Ocean analysis products and climate models have also shown the intensifying and poleward shifting of the subtropical WBC including the Agulhas Current due to long term global warming trends (Yang et al., 2016).

1.2 The Agulhas Current and its sources

As a result of its complex dynamics, the Agulhas Current system with a mean transport of approximately 70 to 72Sv (Sv= $10^6\ m^{-3}\ s^{-1}$) (Bryden and Beal, 2001; Bryden et al., 2005) has received much attention and is therefore the subject of an unprecedented international research effort (Bornmann and Lutjeharms, 2010). The Agulhas Current, which is commonly known as the strongest WBC of the Southern Hemisphere (Lutjeharms 2006; Bryden et al., 2005), flows along the east coast of the southern tip of Africa and constitutes the western boundary of the wind driven, anticyclonic gyre of the South Indian Ocean (Ruitjer et al., 1999). The current is distinctly characterized by both northern (approx. 27° to 33°S) and southern (approx. 33° to 36°S) sections, which equally have an influence on the ocean circulation around South Africa. The northern part of the Agulhas Current has been documented as coherent, stable and well defined due to the continental slope it flows on (Gründlingh, 1983; Bryden et al., 2005; Ruijter, 1999). Its variability is influenced by the occurrence of sporadically solitary meanders known as Natal Pulses (named after region of origin) generated intermittently in the region of the Natal Bight (Rouault and Penven, 2011).

Along the Port Elizabeth coast, the widening of the continental shelf defines the start of the southern Agulhas Current, which flows along the shelf edge of the Agulhas Bank. This region is one of the major nursery and spawning areas of different fish species as seen also in Figure 1.2. The transition of the steepness of the slope influences the behavior of the southern Agulhas Current. In this area the bathymetry increases the instability of the southern Agulhas Current making it turbulent as it develops meanders that flow downstream (Lutjeharms, 2006).

With regard to the primary sources of the Agulhas Current, three main locations are identified: The South Equatorial Current (SEC) that effectively branches to the north and south of the East Madagascar Current (EMC), the southward flow through the Mozambique Channel (MZC) and the recirculation in the South West Indian Ocean subgyre as seen in Figure 1.2 (Lutjeharms and Ansorge., 2001; Bryden et al., 2005; Lutjeharms, 2006). As the SEC flows westwards towards the east coast of Africa, it divides into two branches, at approximately 20°S of Madagascar, forming the northern and southern branches of the EMC. As it approaches Africa, it similarly bifurcates and progresses poleward as the Mozambique Current. Instead of continuing as a coherent current as expected, the flow is characterized rather by a train of large, deep reaching anticyclonic eddies drifting southwards through the channel carrying a mean transport of 17 Sv as documented by in situ (long term moorings) observations (de Ruijter et al., 2004; Ridderinkhof et al., 2010). The EMC flows southward as an intense western boundary current along the east coast of Madagascar (Lutjeharms et al., 1981). On approaching the southern tip of Madagascar, the EMC forms part of the Subtropical gyre system of the South Indian Ocean (Stramma and Lutjeharms, 1997). Here cyclonic

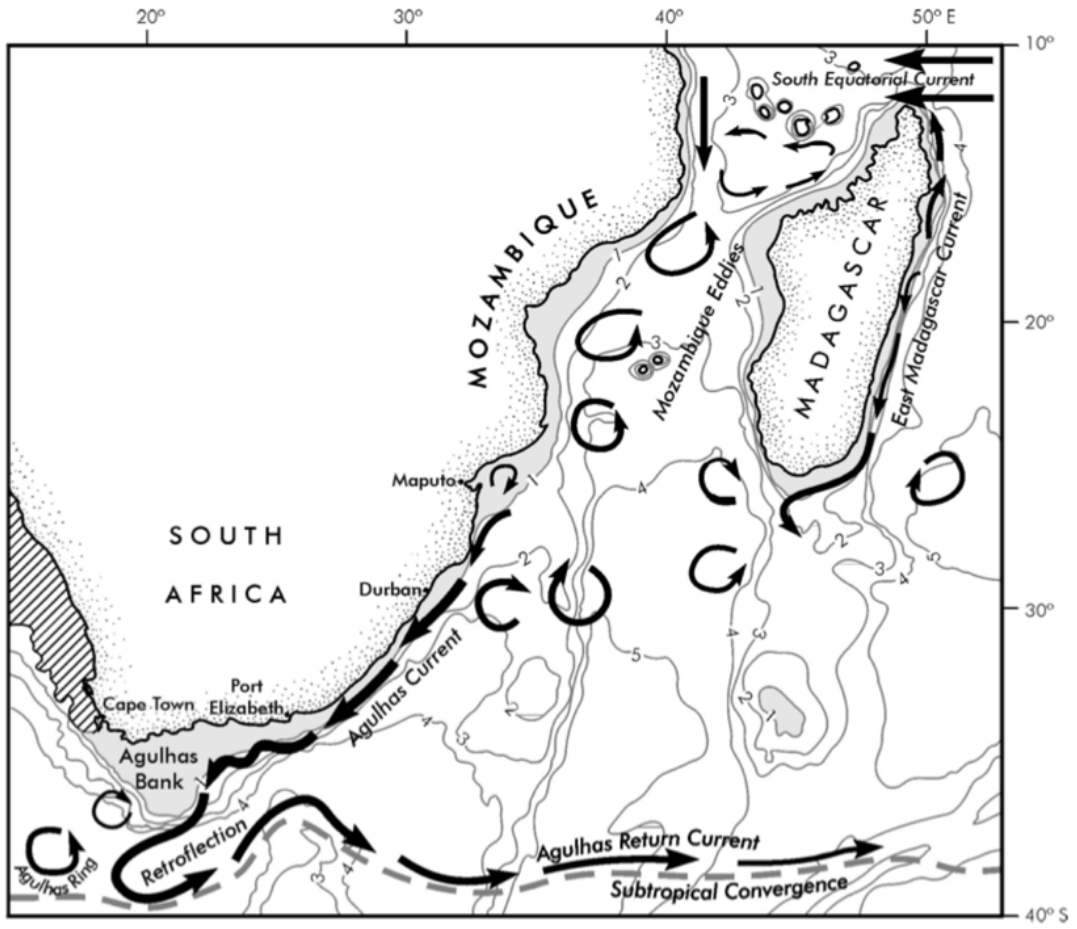

FIGURE 1.2: Schematic showing the basic salient features of the Greater Agulhas Current system: The East Madagascar Current (EMC), South Equatorial Current (SEC) and Mozambique Channel (MC), represent the source regions upstream. The Agulhas Current, Retroflection, Leakage, Agulhas Return Current and Subtropical Convergence downstream. Expressed in km in the background is the bathymetric contours. Currents are indicated using arrows and mesoscale eddies are portrayed by arced shaped features. Adapted from (Lutjeharms, 2006).

and anticyclonic eddies are generated as a result of the EMC Retroflection and propagate towards the Agulhas Current (Lutjeharms et al., 1891).

One of the primary roles of the Agulhas Current is to transport ocean water and its biota into the southern part of the southwest Indian Ocean thereby influencing the ocean´s dynamics and ecology (Lutjeharms and de Ruijter, 1996). The Agulhas Current generates a coastal upwelling at the Agulhas Bank and carries a large body which influences the distribution of pelagic species through advection (Lutjeharms, 2006). The Agulhas Current, driven by the wind field over neighboring basins (You, 2007), also has a profound influence on the weather and climate around South Africa (Lutjeharms, 2006). The Agulhas Current air-sea interactions supports fluctuations of air-sea fluxes associated with the Retroflection and Agulhas Return Current (Rouault, 2009).

1.3 The Agulhas Current Retroflection

Subsequent to the separation of the Agulhas Current from the continental shelf is the retroflection and leakage (Beal and Biastoch, 2010). As the Agulhas Current continues to flow along the east coast of South Africa, it turns back on itself forming an anticyclonic loop as seen in Figure 1.3 (Beal et al., 2011) with a diameter of about 300 to 400 km (Lutjeharms and van Ballegooyen, 1988). This anticyclonic loop is known as the Agulhas Retroflection and potentially sheds rings, eddies and filaments of the Agulhas Current water into the Atlantic at depths of more than 2000 m (Boebel et al., 2003; Gordon et al., 1992). The geographical morphology of the African continent has an influence on the trajectory of the Agulhas Current. The current progressively loops back eastward to rejoin the Sverdrup gyre as it is governed by the large scale wind stress curl (Beal and Biastoch, 2010). The retroflection also forms a western closure of the South Indian Ocean. As a result of the dynamics and instability in this region, the Agulhas Retroflection furthermore contributes to the transport of warm saline water from the South Indian gyre into the South Atlantic through eddies and filaments via the Agulhas leakage (Lutjeharms, 2006). The features that have been implicated in generating disturbances in the Agulhas Current potentially affect the Indo-Atlantic inter-ocean exchange south of Africa (Schouten et al., 2002).

1.4 The Agulhas Leakage

The Indian Ocean waters that are injected from the Agulhas Retroflection and continue into the Atlantic Ocean where they are retained are altogether known as the Agulhas leakage (Loveday, 2014). A number of oceanographic studies have documented an increasing awareness of the influence of the Agulhas leakage as a key component in the global climate system (Beal and Biastoch, 2010; Jury and Walker, 1988; Bornman and Lutjeharms, 2010). Motivated by recent paleodata that suggests the Agulhas Current has an influence on the AMOC, variations observed in the Agulhas leakage may have an influence on the resumption of the AMOC and the rise in CO_2 (Beal et al., 2011; Peeters et al., 2004). Variations of the turbulent leakage have a substantial impact on the overall ocean circulation. For instance, Morris et al., (2017) document that the injection of Indian Ocean water masses into the Atlantic Ocean has an overall influence on balancing the AMOC. The shutdown of the Agulhas leakage has been associated with extreme glacial periods while a robust increment has antecedent shifts towards interglacials (Beal et al., 2011).

Model outputs have shown possible anthropogenically induced shifts in wind patterns over the Southern Hemisphere (Bornmann and Lutjeharms, 2010). Over longer time scales the variability of the leakage has been associated with large scale wind fields such as the Southern Hemisphere westerly winds. Essentially, variability associated with

the westerlies is likely to impact the gateway between the African continent and the Subtropical Front (STF); a northward shift of the westerlies has a potential to reduce the leakage. Conversely, a southward shift of the westerly winds expands the gateway increasing the leakage from the Indian to Atlantic Ocean (Biastoch et al., 2009; de Ruijter., 1982).

The Agulhas leakage also forms a thermohaline link between both the Indian and Atlantic Ocean connecting the Agulhas Current system with the upper branch of the AMOC through a warm water route (Gordon 1986; Beal et al., 2011). In addition, a number of studies argue that the upstream inertia results in an increase in the Agulhas leakage (Van Sebille et al., 2009). In contrast (Rouault et al., 2009), have argued that the strength of the Agulhas leakage has been influenced rather by the Agulhas Current transport. A proportion of the Agulhas leakage remains in the South Atlantic Subtropical gyre, while some of it ends up in the supergyre and subsequently circulates into the Indo-Pacific region via the South Atlantic Current. The remaining Agulhas Leakage then feeds into the upper surface arm of the global AMOC crossing the equator (Beal et al., 2011).

1.5 The Agulhas Return Current

The Agulhas Return Current (ARC) is significantly modified south of Africa through contributions from the Agulhas Current (Lutjeharms and Ansorge, 2001). A synthesis of available hydrographic data by Boebel et al., (2003) has documented the ARC as a spatially and temporally variable current of about 60 to 80 km in width. Located nominally at 39°S, it exhibits velocity measurements of up to 2 m/s. Although the degree of variability of the ARC has to date not been determined with reliability (Lutjeharms and Ansorge, 2001), Belkin and Gordon (1996) show that it extends as far east as 72°E. The general motion of the ARC is zonal (Gründlingh, 1979; Daniault and Ménard, 1985; Hofmann, 1985) with bottom topography influencing extensive meridional excursions along its path (Darbyshire, 1972; Lutjeharms and Van Ballegooyen, 1984). Equally important to the Agulhas Current, the ARC also plays a vital role in influencing the climate around South Africa.

1.6 The Agulhas Current flow regime

Considering the general overview of the Agulhas Current system, the variant Agulhas Current and its sources, Agulhas Retroflection, Agulhas leakage and Agulhas Return Current occur interdependently to form an Agulhas Current system. This system functions effectively by integrating all the physical and thermodynamic processes with the

primary goal of transporting momentum, nutrients, heat and salt poleward and potentially have a profound impact on long term trends in the climate system (Benny et al., 2015).

Increasingly, the scientific community has drawn their attention to this system´s integration of the inter oceanic exchange between the Atlantic and Indian ocean. Warm and salty water leaks (Agulhas leakage) from the Indian to the Atlantic Ocean via the Agulhas rings supplied by the Agulhas Current during the retroflection off the continental shelf break close to the southern tip of Africa (Gründlingh et al., 1983). A body of research has also focused on documenting the path and variability within the system (Boebel et al., 2003) and the principal pathways of exchange within the wide basin scale (Benny et al., 2015).

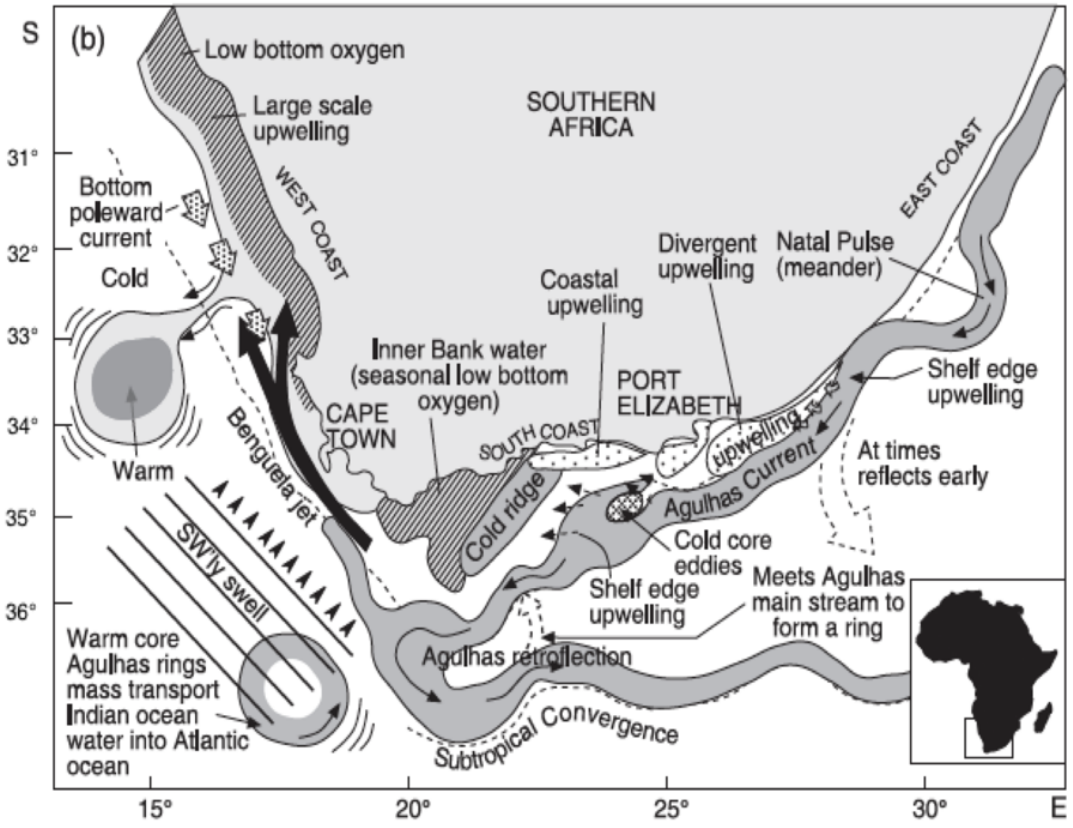

FIGURE 1.3: Features of the large scale circulation showing the complexity and variability of the Agulhas Current system. This includes the onset of small meanders (Natal Pulse - along the east coast), upwelling along the Agulhas Current and divergence of the current axis from the coast, Agulhas Retroflection and downstream meander of the Agulhas Return Current located along the Plateau (Adapted from Robertson, 2005).

The variability observed within the Agulhas leakage plays an important role in glacial terminations and the timing of interhemispheric climate change (Peeters et al., 2004). From its genesis, the Agulhas Current system has been perceived instrumental for moving Indian waters towards the South Atlantic Ocean (Gordon, 1985) and evidence is seen

through the spawning of Agulhas rings and Agulhas filaments at the Agulhas Retroflection with mean heat loss of down to 200 W/m^2 (Lutjeharms, 2006). These Agulhas rings migrate into the Cape basin as they split, amalgamate and rapidly spin down near the southern terminus of the Agulhas Current. The juxtaposition between the (Lutjeharms and Ansorge, 2001) Return Current and the weak front Subtropical Convergence as seen in Figure 1.3 also contributes to the dynamic flow in this region as it periodically sheds eddies (Boebel et al., 2003). Such processes occur south of Africa where the Agulhas Return Current lies north of the Subtropical Convergence. Paramount modifications of water masses have been observed in this region as a result of not only the air-sea interactions, but also the continued process of different water bodies mixing. Frontal characteristics of the less intense front are therefore potentially strengthened by the Agulhas Return Current (Lutjeharms and Ansorge., 2001). The Agulhas Current as a western intensification boundary system therefore plays an important role in connecting the Agulhas Current, Agulhas Retroflection, Agulhas leakage and the Agulhas Return Current´s physical properties along with associated mesoscale processes.

1.7 What is the role of mesoscale variability?

Mesoscale features are identified as dominant reservoirs of kinetic energy and prominent sources of flow variability throughout the global ocean (Gille, 2003; Meredith et al., 2006; McWilliams, 2016). The nomenclature behind these oceanographic features is due to their large spatial horizontal scale of tens of kilometers from approximately 50 to 100 km and an evolutionary period of weeks from 10 to 100 days depending on their location (Schiermeier, 2007; Chelton et al., 2011; McWilliams, 2016). Previous research efforts within the Agulhas Current system, were primarily directed towards understanding mesoscale features and their role in climate change and ocean circulation processes (Hall and Lutjeharms, 2010; Backeberg et al., 2012; Lamont et al., 2014; Tandeo et al., 2014). Through their physical processes, these mesoscale features provide a vehicle for the transport of heat and dissolved gases such as CO_2, which potentially enable outgassing or uptake of CO_2 gas at surface or subsurface layers of the ocean (Melato, 2012). There is also a strong connection for nutrients as underlined by Lévy et al., (2012). Additionally, the intensification of the mesoscale variability has a potential downstream implication for the Agulhas Current and an influence on the South Atlantic Ocean leakage (Backeberg et al., 2012). This is influenced by the connection with upstream Agulhas sources (SEC, MZC and EMC), which potentially increase eddy properties (eddy radii, amplitude and westward propagation velocities) and volume transport (de Ruitjer et al., 2004; Shouten et al., 2002; Siedler et al., 2009). Mesoscale variability is known to be responsible for more than 95% of the oceanic kinetic energy (Munk, 2000). Geographical variation observed within mesoscale features is through their size, radii, and amplitude

while a minor seasonal modulation is documented in most locations as inferred from satellite altimetry respectively (McWilliams, 2016).

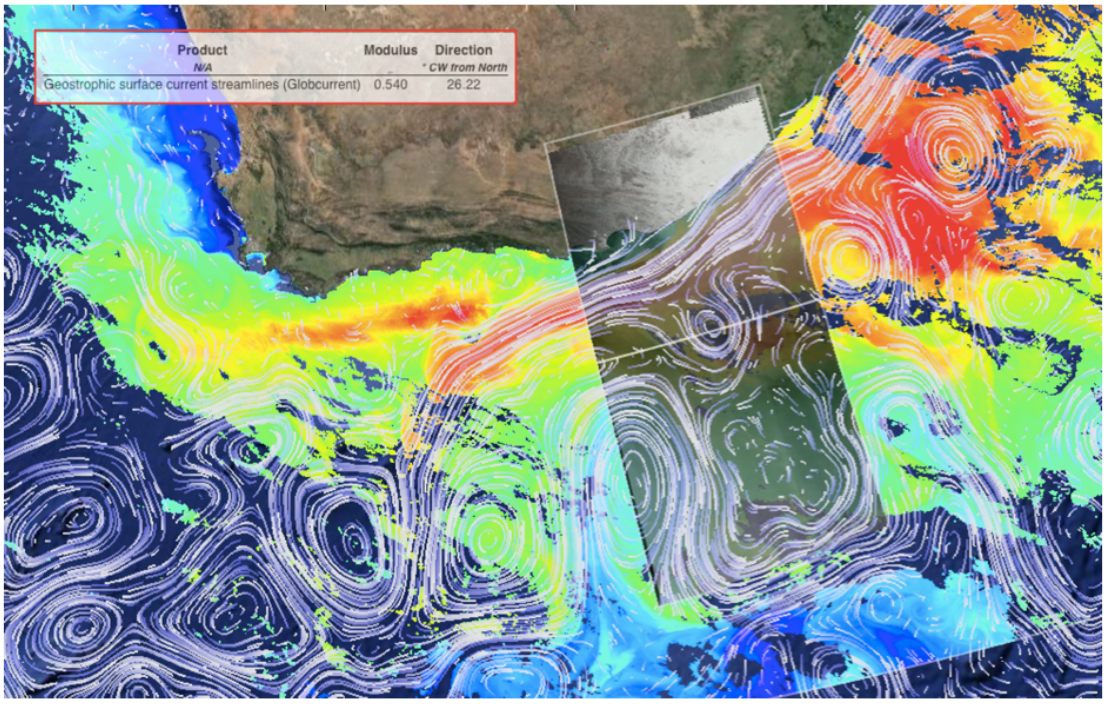

FIGURE 1.4: Schematic showing the ocean surface dynamics at the southern tip of Africa: The geostrophic surface current streamlines (white lines) overlaid indicate the flow variability emerging from mesoscale features such as the current (Agulhas Current and Agulhas Return Current), eddy corridor consisting of both cyclonic and anticyclonic eddies and meandering of the current with sea surface temperature in the background (indicated by the red, blue green interpolation) from (www.ocean data lab.com).

The ability to accurately sample the ocean using satellites has been difficult due to limited global coverage (Munk, 2000). Contemporary improvements in remote sensing have enabled multi mission mapping techniques of these altimeters to accurately resolve mesoscale variability (Chelton et al., 2011). This robust technique measures synoptic patterns of mesoscale features that include current meandering, eddy shedding, front displacements and variations observed in speed and direction (propagation velocities) of boundary currents (Lutjeharms and Cooper, 1996; Ducet et al., 2000; Backeberg et al., 2012).

1.8 Mesoscale variability leading to submesoscale features

Submesoscale features on the surface of the ocean are defined as intermediate horizontal scale (1 km) flow structures that appear in the form of density fronts and filaments, topographic wakes and persistently occurring coherent vortices or swirls (McWilliams, 2006) as seen in Figure 1.4. Their operational name is defined from mesoscale features and they emerge spontaneously in simulations of both mesoscale eddies and strong

currents. These submesoscale features like the mesoscale eddies are essential as they provide a conduit of dynamical energy transfer and biota towards microscale dissipation and diapycnal mixing as shown in Figure 1.5. It is therefore important to have an equivocal understanding of the various scales of variability, flowing from the mean circulation through the turbulent motions emerging from mesoscale to submesoscale features (Toole and McDougall, 2001; Ridgway and Dunn, 2003).

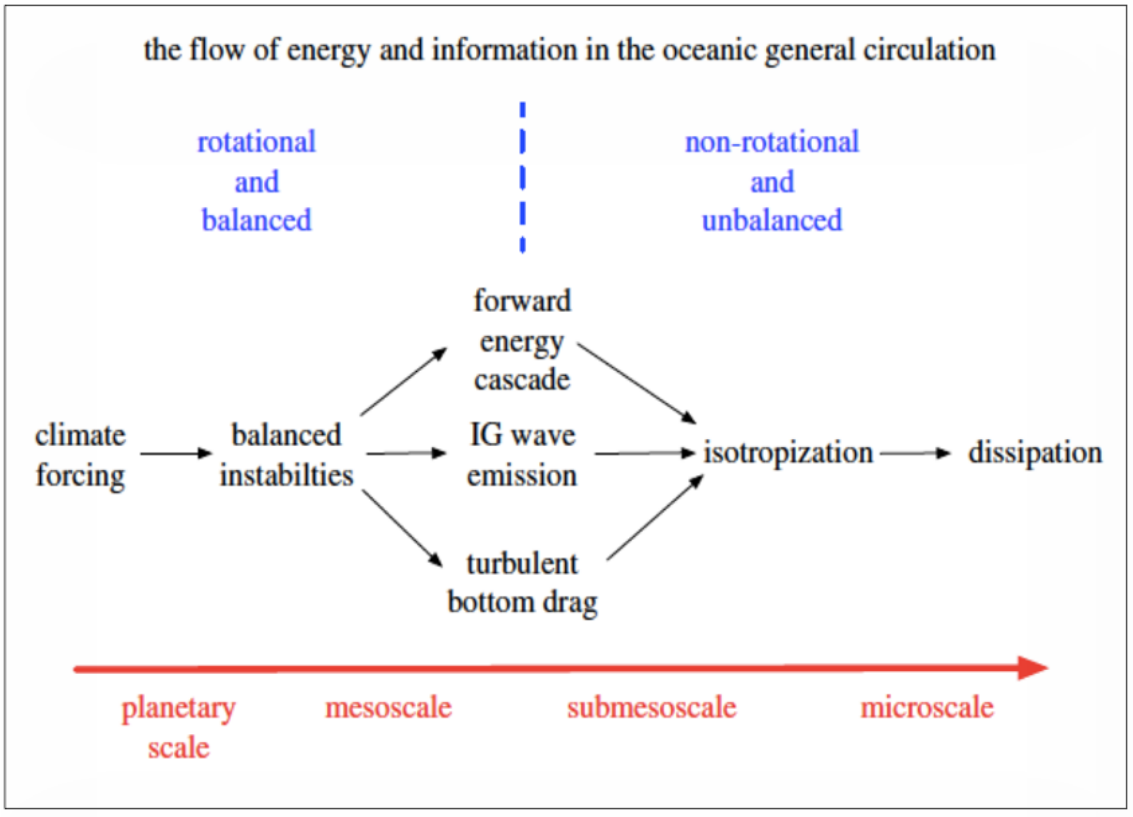

FIGURE 1.5: Shows the stages in the general ocean circulation from planetary-scale forcing to microscale dissipation and mixing within the submesoscale regime. Adapted from (McWilliams, 2016).

A quantitative outlook on the size of submesoscale features is essential: The length of the horizontal scale is between 0.1 and 10 km and their height is between 0.01 and 1 km in the vertical scale and a temporal evolutionary scale of hours and days. According to McWilliams (2016), the size of submesoscale features provide an observational challenge that unfortunately delays an appreciation of their ubiquitous nature across the ocean surface. First and foremost, they are often either too large to be detected accurately from shipboard instruments or low resolution satellites. Incidentally they are also too small as shown in Figure 2.3 and as a result of their advective nature they are rapidly dynamic and evolve over time, making it difficult to enable precise ship surveys. Additionally, they provide a small footprint for majority of remote sensing satellites. To date, there are no comparable global measurements of submesoscale features and a central problem is documented in meteorological and other geophysical forecasts in model initialization from measurements. Hence one of the primary scientific rationales for the development of

satellite missions such as Surface Water Ocean and Topography (SWOT) (to be launched in 2020) is to establish high resolution, wide swath altimetry measurements of surface water and ocean topography in order to make fundamental advances in understanding the processes underlying small scale features (inclusive of mesoscales) and sea surface salinity variability (Boutin et al., 2016). The general ocean circulation of submesoscale features is largely influenced by fluxes of momentum, heat, water and differences in planetary scales essentially (McWilliams, 2016). SWOT therefore envisions to contribute unique global observations to allow characterization of different regimes in different regions and seasons (Klein et al., 2015).

1.9 Rationale of the Crossroad transect

Warming has been identified across the Agulhas Current system as a response of increased wind stress curl in the South Indian Ocean (Rouault et al., 2009). Rouault et al., (2009) show that these warm sea surface temperatures approximate down to 0.7°C per decade of warming within the system. Similarly, Rouault et al., (2009) show that higher sea surface temperatures are observed at the Agulhas Retroflection due to the expected increase in kinetic energy linked with the transport south of Madagascar. The upstream perturbations have a potential to influence the characteristics or representation of the salient features downstream such as the Agulhas rings including their drift path (Biastoch et al., 2008). A program within the South Atlantic Meridional Overturning Circulation (SAMOC) has a core objective of linking the south east Atlantic with the south west Indian Ocean. Between 2004 and 2012, the GoodHope line has been the only South African monitoring cruise line spanning the Agulhas leakage region and Antarctic Circumpolar Belt. Although the line enables the quantification of heat, salt and volume exchange between the Indian and Atlantic Ocean, the difference in fluxes between the westward flowing Agulhas Current and the eastward zonal Agulhas Return Current remains rudimentary (Ansorge, 2013).

With an increased range of uncertainty and contradictions observed within the system, extensive research is required to unequivocally understand the Agulhas Current system and dynamics thereof. Evidence of progress and development in terms of research within the Agulhas system has been observed. The evolution was documented by (Biastoch and Krauss, 1999) who contended that the identification of source regions of the Agulhas Current was restricted and that the extent of gaps found in the role played by the Mozambique Channel was vast. Sparse hydrographic observations were unable to clearly reproduce a consistent representation of the Agulhas Current. And therefore, innovative approaches are still required for model development for a better analysis from basic to complex oceanographic phenomenon such as the Agulhas Current system considering all scales from a global (Beal and Biastoch, 2010; Beal et al., 2011), regional (Rouault

et al., 2009; Halo et al., 2014) to local (Backeberg et al., 2012; Backeberg et al., 2014) extent.

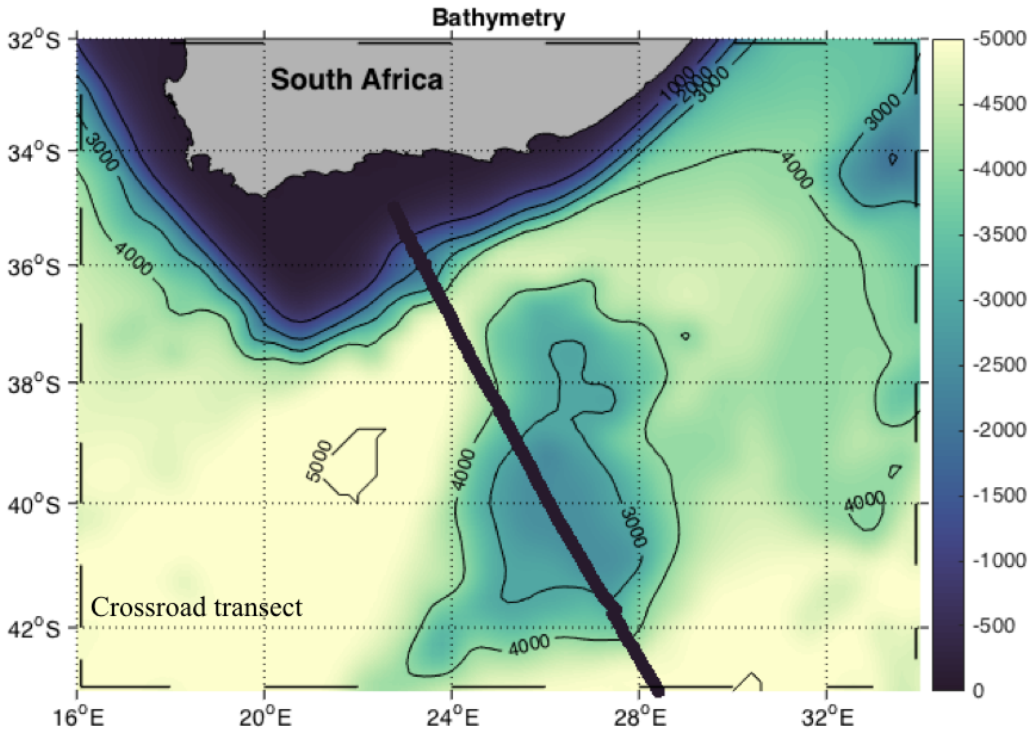

FIGURE 1.6: Map showing the bathymetry across the Crossroad transect south of Africa. The blue line represents monitoring route occupied annually during the voyage from 35°S to approximately 42°S. The isobaths contour interval observed is 1000 m.

A dedicated cruise line known as the Crossroad transect has been established. Sampling along this route commenced in 2013 with the overarching goal of studying the long term trends in ocean fluxes. The primary goal is to fundamentally establish the nature of the system, the warming of currents and their potential impact on local climate around South Africa (Ansorge, 2013). The monitoring line as seen in Figure 1.6 lies at a location that allows measurements of both the Agulhas Current and its return flow as they are simultaneously constrained by the Agulhas Plateau and coincide with the N198 altimetry track (Cooper, 2014). The motivation behind the establishment of the Crossroad transect was to better understand the Agulhas Current system across the Agulhas Plateau by integrating annual satellite altimetry across the monitoring route (Ansorge, 2013). The SA Agulhas II (dedicated to a South African Icon, Mrs. Mariam Makeba) annually embarks on a voyage from Marion Island enabling collection of hydrographic data for scientific research community.

The need to extend all ocean observations from cruises is to bring in satellite imagery. The warming of the Agulhas Current as documented by Rouault et al., (2009) has focused research attention on the Agulhas system. Considering the variability observed along this region the study aims to investigate the dynamic nature of the Agulhas system and the gaps often overlooked between small and large scales features. Despite the 3 years (from 2013 to 2015) of data currently available, a short term interannual variation between these years is still considered. Although short term interannual variability is examined in the study, the seasonal variation along the transect remains a limitation. This study therefore attempts to understand the variability across the Crossroad transect using 3 years of hydrographic data. Fundamental to understanding the Agulhas system, is determining the role played by small scale features that form part of the local, regional and global ocean circulation.

Chapter 2

Introduction

2.1 Context and motivation

The Agulhas Current as it flows southwestward along the eastern coast of South Africa, retroflects along the Agulhas Bank and forms an eastward continuation known as the Agulhas Return Current (Beal et al., 2011; Lutjeharms, 2006), allowing approximately 90% of its water mass transport into the South Indian Ocean (Whittle et al., 2008). This system has been studied extensively due to its dynamic nature and general flow pattern (Dencausse et al., 2010). To date, the trajectory of the Agulhas Return Current has not been determined with accuracy, although it is known to be variable (Lutjeharms and Ansorge, 2001). Different studies have also shown the increase in warming of the Agulhas Current, along with the fluctuation of air sea fluxes such as latent and sensible heat fluxes, which increase 3 to 5 times over sea surface temperature fronts linked with the Agulhas Current, Retroflection and Return Current (Beal et al., 2011; Rouault et al., 2000). Consequently, the variation associated with the Agulhas system contributes to the impact on the climate of South Africa (Rouault et al., 2009), leading to environmental, poverty, health, and safety challenges on different disciplines (Morris et al., 2017). Furthermore, the Agulhas leakage, which forms part of the Agulhas system injects some of its water masses into the Atlantic Ocean and has increased since the 1980s (Rouault et al., 2009; Biastoch et al., 2008a).

Within the Agulhas Current system different components functioning independently are observed at different scales including, but not limited to the basin and mesoscale features. On a regional scale, Lutjeharms (2006), put forward that the Agulhas Current has a direct influence on the oceanography associated with continental shelf through a range of the mesoscale and submesoscale processes. Therefore, to understand better the variability associated with the Agulhas Current system, different hydrographic datasets collected along the Crossroad tranect are used. Sampling along the Crossroad transect was commenced in 2013 with the primary goal of analysing both the Agulhas Current

and the Agulhas Return Current. However, data collected along this route remains incomplete. For instance, to date, there is no evidence of high resolution glider data to infer on the biogeochemical measurements that influence the mesoscale and submesoscale features along the Crossroad transect and this essentially remains one of the limitations of the study.

2.2 Why study small scale such as mesoscale and submesoscale features along the Crossroad Transect?

Figure 2.1 shows the importance of scales in time and space, the connection and dependence of processes on one another. As a result of the prominent energy flows involved within small scale dynamics, processes such as water cycle are coupled with the global energy balance. Previous studies have shown that ocean-atmosphere interactions influence the regional climate system through radiative heat balance (Trenberth et al., 2009; Stephens et al., 2012; L'Ecuyer et al., 2015). These features further continue to stir large scale sea surface temperature fields as mentioned by Tandeo et al., (2014). Understanding better the role of climate change creates an awareness of important intensification of regional floods and droughts and how they provide vast potential impacts on distinct societies (Köhler, 2015). Though knowledge of these mesoscale features remains rudimentary across the Crossroad transect, previous research studies have documented that mesoscale eddies have a central role in upwelling deep, nutrient-rich waters into the oceans´ euphotic zone, which potentially influences an abrupt growth of autotrophs such as phytoplankton (Quartly and Srokosz, 2004). Both mesoscale and submesoscale features enable researchers to quantify the oceanographic conditions within distinct regions and therefore conclude on different physical ocean properties such as temperature and salinity, which altogether provide inference on the density state of different water bodies (L'Hegaret et al., 2016). The near surface temperature and salinity data collected from different oceanographic instruments are used to compute the horizontal temperature, salinity and density fluctuations (Kolodziejczyk et al., 2015). These properties of the horizontal mixed layer vary significantly as a function of location, season and as a function of both spatial and temporal scales and will be discussed further in chapter 5.

Dong et al., (2014) assert that surface thermohaline structures are primarily driven by baroclinic instabilities (measurement of the misalignment of the gradient of pressure from the gradient of density in a fluid) of currents located at frontal regions of mesoscale levels, which are known as eddies. These features altogether play a fundamental role of potential energy conversion in the upper ocean (Kolodziejczyk et al., 2015). Additionally, these mesoscale processes have an impact on biological dynamics. They impact phytoplankton growth and increase productivity by modulating the vertical supply of nutrients into the euphotic zone and regulate the strength of vertical mixing (Lévy et al., 2012). Furthermore, Figure 2.1 mainly shows the importance of scales in time and

space, and the connection and dependence of processes on one another. To reiterate, it is important to understand the variation along the Crossroad transect at different scales as it affects the characterisation of different water properties.

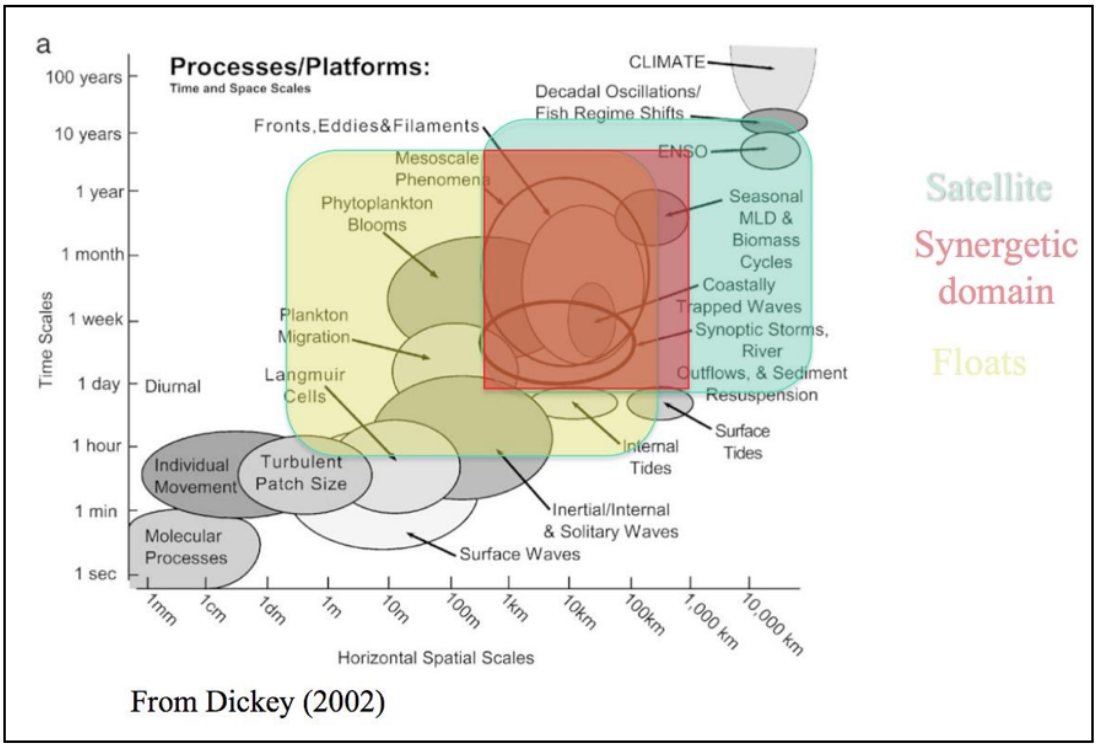

FIGURE 2.1: A schematic of temporal-horizontal space scale showing physical and biological platforms over time. The approximate horizontal and temporal sampling domain capabilities of various platforms are represented in rectangles. These includes satellites and floats as shown in different colors. Adapted from Dickey (2002).

2.2.1 Why consider sea surface salinity observations?

Salinity is one of the variables that play an important role in the thermohaline circulation (Reul et al., 2013). However, fundamental problems of physical oceanography include quantifying salinity variations in the ocean and their underlying processes. Morrisset et al., (2012) document that sea surface salinity data derived from satellite are often less erroneous and the variations thereof on both seasonal and interannual timescales are high. Satellite missions have an objective of better resolving the observed variability in sea surface salinity estimates with an accuracy of 0.1 to 0.2 psu over Global Ocean Data Assimilation Experiment (GODAE) scales of 100 km over 1 to 2 months and 10 days (Reul et al., 2014). Variations in salinity are an expression of disparity in the transport of freshwater and together with temperature these variations have a major influence on the density of sea water and ocean circulation (Köhler, 2015). Zhu et al., (2014) put forward that the variations play a role in the maintenance of the climate through its effects on horizontal pressure gradient, stratification and the equatorial thermocline.

Historically, salinity has been one of the most under-sampled quantities hence the elusiveness in detailed knowledge regarding long term ocean salinity changes. Maes et al., (2014) contend that the large scale variability observed in sea surface salinity can now be examined with unprecedented space and time sampling. Additionally, measurements of the distribution of altimetry derived sea height and temperature at the surface present a wealth of information regarding ocean circulation. Furthermore, recent studies have focused on the synergy between different water properties including temperature and salinity at surface and subsurface layers in order to highlight the correlation between different fields for the full comprehension of coupled dynamics. Despite recent efforts, small scale variability in salinity remains a challenge and more knowledge is essential (Boutin et al., 2016) .

2.3 Objectives, approach and outline of the study

The Agulhas Current system is known as a complex oceanographic system and has a potential influence on both regional and global climate (Lutjeharms, 2006; Beal et al., 2011). Examining both the basin and mesoscale features across the Crossroad transect given the inherent advantage of satellite remote sensing and access to different in situ datasets forms the main objective of the study. On the other hand, the aim is to investigate and compare distinctive water properties using different ocean instruments, which include the Conductivity Temperature and Depth (CTD), Thermosalinograph (TSG) and Shipboard Acoustic Doppler Current Profiler (SADCP). In addition to using these instruments, different resolutions highlight different properties, allowing an analysis of diverse range of scales from basin to submesoscale. This study similarly, provides an abundance in ocean observations allowing a detailed perspective on different ocean variables that include surface temperature, salinity, velocity and geostrophic velocity measured at both surface and subsurface layers. Although submesoscale features are not the focus of the study, they will be discussed briefly due to the role they play in contributing to the overall large ocean circulation (Krug et al., 2017; McWilliams, 2016; Kolodziejczyk et al., 2015). The study altogether aims to achieve a better understanding of the variability along the Crossroad transect using 3 years of hydrographic data. In order to achieve the above mentioned objectives, as part of the research goal of this study the following three key questions will be investigated:

1. What basin scale circulation features do we observe across the Crossroad transect?

To answer this question, this study will evaluate the basin scale features identified along the Crossroad transect with the anticipation of demonstrating the altimetry and in situ data. Particular emphasis will focus on the interdependent components of the Agulhas Current system along the transect at both surace and subsurface layers. Despite the

limitations of satellite observations, a synergy of in situ data is implemented allowing a further understanding of the variability along the Crossroad transect.

2. How do observations of basin scale and mesoscale features differ when using different datasets?

The impact of the study investigates different scale features (currents, fronts, eddies, meanders and filaments) through integrating remote sensing satellite sensors with in situ measurements in order to fully understand spatio-temporal variability across the Crossroad transect. This is done by highlighting what is missing from one dataset that can be explained by other datasets including both hydrographic and altimetry data (Maes et al., 2013).

3. Are there interannual similarities and differences in the basin and mesoscale variability observed along the Crossroad transect between 2013 and 2015?

Past observational research was unable to show a seasonal cycle of the Agulhas Current system (Gründlingh, 1983; Bryden et al., 2005). Conversely, regional models exhibit seasonality in the transport of the Agulhas Current (Lutjeharms, 2006). Although altimetry and in situ datasets have to date not been able to provide such evidence along the Crossroad transect, a short term interannual variation is determined. This is done by considering the sea surface temperature and salinity measurements from the thermosalinograph along the transect and comparing the patterns observed on different scales.

An overview of the salient features and dynamics of the greater Agulhas Current system is provided in Chapter 1, including the sources of the Agulhas system. In addition the role of the mesoscale variability leading to submesoscale features is briefly presented with the aim of defining some of the key driving processes of variability within the Agulhas Current system. An introduction of the data and methods including hydrographic sampling is provided focusing on ship based in situ datasets and satellite remote sensing in Chapter 3. Furthermore, as seen in Chapter 4 results are presented with measurements compared to assist in understanding the variability across the Crossroad transect using 3 years of hydrographic data. Chapter 5 then highlights interesting trends, patterns and features often overlooked in the data. Finally, a summary of the research is drawn in Chapter 6 including potential future research recommendations and a perspective of the study.

Chapter 3

Data and Methods

3.1 Study region and hydrographic sampling

The study area covers the ocean domain around southern Africa from 32° to 43°S and 16° to 32°E as seen in Figure 3.1.

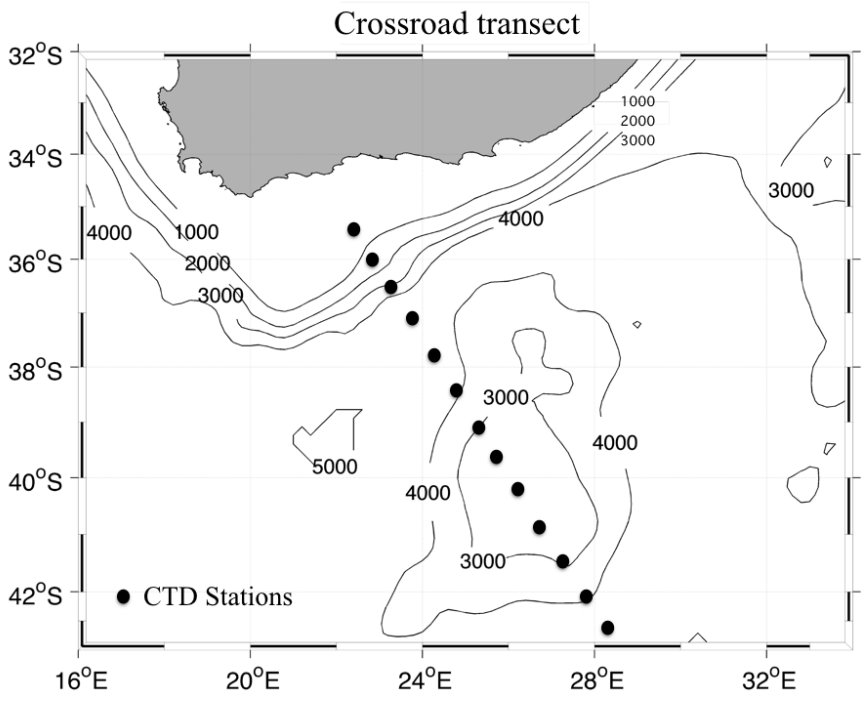

FIGURE 3.1: Map showing the bathymetry and Crossroad transect. Isobaths indicate the bathymetry with a contour interval of 1000 m. The black dots represent the CTD stations. Across the transect the Agulhas Plateau is observed as indicated by the isobaths ranging between 3000 and 4000 m.

The geographical domain displayed in Figure 3.1 covers a large extension of the Agulhas Current system around southern Africa. The aim of the Crossroad transect is to establish a monitoring route that will provide detailed hydrographic data on the structure of both the Agulhas Current and Agulhas Return Current. This chapter will focus on the ship based datasets including shipboard ADCP, TSG and CTD and satellite remote sensing products from Aquarius, SMOS and Aviso will be explained briefly.

3.2 Ship-based in situ datasets

The Crossroad transect is now on its 4^{th} year of sampling. The overarching aim is to achieve the long term trend in inter-oceanic fluxes and to establish the nature of warming currents and their impact on local climate south of Africa (Ansorge et al., 2013). The purpose is to present annual analysis of the information collected along the Crossroad transect during the return voyage from Marion Island to Cape Town. Onboard the vessel, underway data was collected from various oceanographic instruments recorded on the Scientific Data System (SDS). Maes et al., (2013) contend that quality controlled in situ observations are important in terms of calibration and validation of satellite measurements. The instruments employed in the study include the CTD, which measures temperature, conductivity and depth, TSG measuring temperature and salinity at the surface of the ocean and SADCP measuring the current from near surface to approximately 500 m.

3.2.1 Shipboard Acoustic Doppler Current Profiler (ADCP) measurements

During each voyage, the vessels keel mounted 75 kHz Teledyne RD Instrument SADCP was set to collect data. Data was gathered using the Teledyne RDI VMDAS (version 1.46) software. The instrument was adjusted to accumulate data for approximately 60 bins, with a bin size of 8 m to a total depth of 560 m. The instrument alignment correction in relation to the vessel was set to -46°. Short Term Average (STA) data, using a 3 minute average from the ADCP was processed down to a maximum depth of 501 m. The gathered data was converted into a spreadsheet using an extraction function from Aqua Vision ViSea DAS and ViSea DPS software. All velocity data is measured in m/s (van den Berg, 2015).

3.2.2 Thermosalinograph (TSG) measurements

For the duration of the voyages from 2013 to 2015, the TSG system was run for the collection of underway temperature and salinity data. The instrument receives sea water

from the onboard sea water supply manifold in the scientific laboratory with seawater being pumped from the sea chest located in the engine room close to the laboratory. The TSG in situ data represents the instantaneous point wise measurements sampled once along track and averaged along track nominally (Köhler, 2015).

3.2.3 Conductivity Temperature and Depth (CTD) measurements

Onboard the vessel, CTD casts were lowered profiling temperature, salinity and fluorescence from near surface to depths of down to 4000 m under strict conditions that the vessel is stationary. A rosette of 12 Niskin bottles was deployed and bottles were closed at standard depths of 5 m, 10 m, 20 m, 50 m, 75 m , 250 m, 1000 m, 1200 m, 1500 m and 2000 m. The study will focus on temperature and salinity profiles down to 2000 m collected from 2013 to 2015. The units of salinity reported in this study are practical salinity units (psu). In 2013 a total of 18 CTD stations were measured from the 10^{th} to 15^{th} of May from 35.5° to 42°S. The Agulhas Current was identified prior to the survey from the Group of High Resolution Sea Surface Temperature (GHRSST) satellite sea surface images. In 2014 a total of 17 full depth CTD stations were deployed from the 10^{th} to 15^{th} of May sampling and collecting data from 35° to 42°S as also seen in Figure 3.1. In 2015, data collection similarly took place during the return cruise from the 2^{nd} to 5^{th} of May stationing at the same region of interest with a total of 19 stations.

3.3 Satellite Remote Sensing

3.3.1 Aquarius and SMOS

Following Martin (2014), the past forty years have advanced the ability of satellites to allow observation and monitoring the global ocean and its overlying atmosphere through vast technological development. Remote sensing is defined as the use of electromagnetic radiation in order to acquire data from the ocean, land and atmosphere without physical contact with the phenomenon being investigated. National Aeronautics and Space Administration (NASA) missions therefore provide precise first space borne measurements of the sea surface salinity to characterize these ocean land interactions with unprecedented space and timing sampling (Maes, 2014). The Soil Moisture and Ocean Salinity (SMOS) and Aquarius satellite are intently considered in this study as they exhibit the main characteristics of the global sea surface salinity, temperature and height distribution (Köhler, 2016). Events such as the Indian Ocean Dipole have also been documented using SMOS data from patterns of salinity variability (Durand et al., 2013).

The SMOS and Aquarius measurement intensity is based on the electromagnetic radiation in the L band with a frequency of approximately 1 to 2 GHz. SMOS was launched

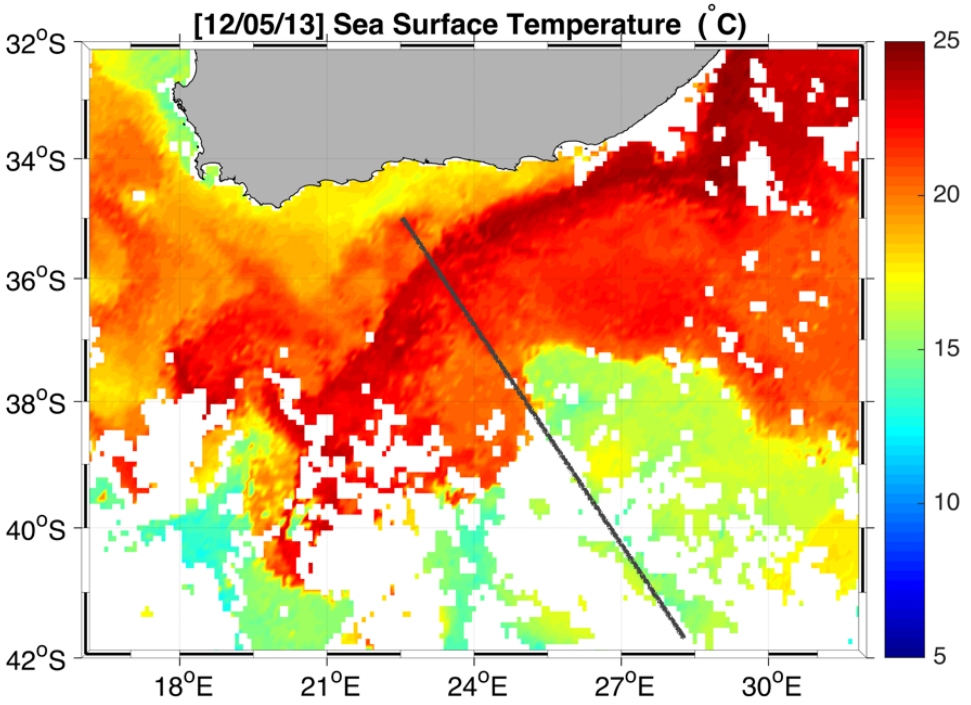

(a)

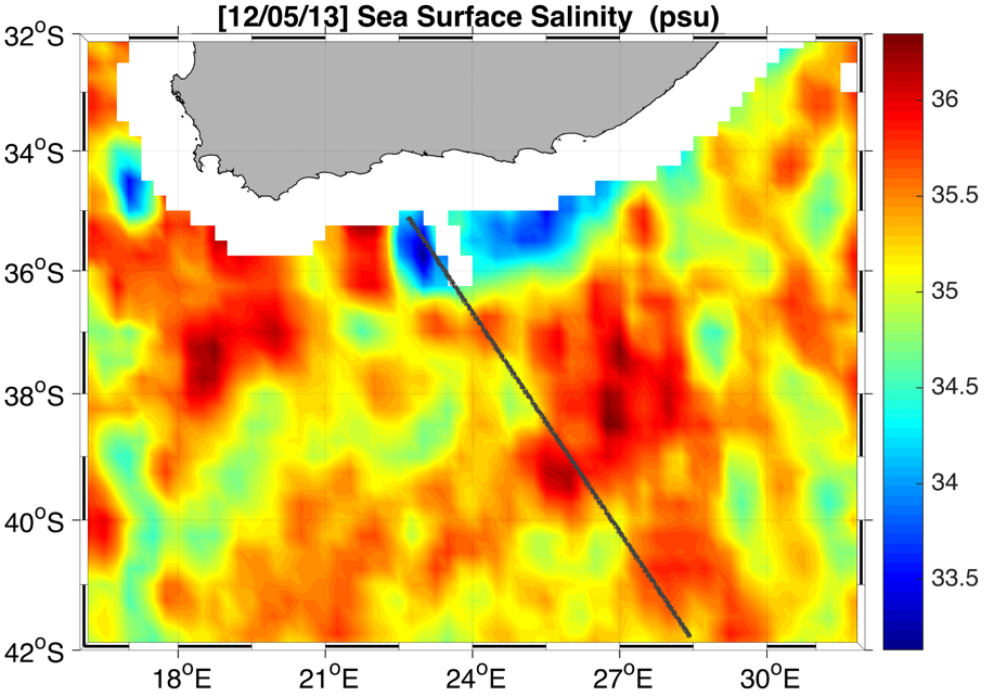

(b)

FIGURE 3.2: Map showing an overview of Sea Surface Temperature (SST) obtained from Aquarius and Sea Surface Salinity (SSS) obtained from SMOS. The black line indicates the Crossroad transect.

	SMOS	**Aquarius/SAC-D**
Instrument	MIRAS	Aquarius
Instrument concept	Passive microwave 2D-interferometer	Passive radiometer and active scatterometer
Orbit	Sun-synchronous	Sun-synchronous
Altitude	763 km	657 km
Frequency	1.43 GHz	1.413 GHz and 1.26 GHz
Spatial resolution	35 km at the center of the FOV with a radiometric accuracy $\approx$ 1.2K	79×94 km for inner beam
Temporal resolution	3 days	7 days

TABLE 3.1: Summary table showing the characteristics of the SMOS and Aquarius satellites. (www.aviso.altimetry.fr).

November 2009 and flies in a sun-synchronous orbit covering the global ocean every 2.7 days. It is a polar orbiting satellite carrying an interferometric radiometer operated at a frequency of 1.4 GHz. A swath of 1000 km is estimated with a nominal spatial resolution of approximately 43 km (Maes, 2014). The advent of SMOS makes it feasible to quantify the assessment of the mechanisms that govern the ocean surface variability and infer on the salinity budget (Durand et al., 2013). The primary objective of SMOS is to remotely sense the moisture of the continental surfaces and surface salinity content of the oceans. The NASA Aquarius instrument on the other hand comprises a passive microwave radiometer in the L band at approximately 1.413 GHz (Aslebagh, 2013). Similarly, Aquarius flies in a sun synchronous polar orbit with a significant difference global coverage of the ocean every 7 days (Köhler, 2016). Figure 3.3 indicates the differences in table format of SMOS and Aquarius.

3.3.2 AVISO

The satellite data used in the study are also obtained from AVISO (Arching, Validation and Interpretation of Satellite Oceanographic). The altimetry results observed in chapter 4 are based on gridded Maps of Absolute Dynamic Topography Heights (MADT-H) obtained from the SSALTO/DUACS data products (www.aviso.altimetry.fr). The products are used to investigate the circulation and the mesoscale activity across the Crossroad transect. The SSALTO/DUACS processing integrates data combined from all altimetry missions: Jason-1, Topex/Poisedon, Evisat, GFO, ERS-1 and 2 (User Handbook Ssalto/Duacs: Mean Sea Level Anomaly (MSLA) and M(ADT) Near-Real Time

and Delayed-Time Products) (Ducet et al., 2000). Therefore, daily sea surface elevation (SSH) products with a spatial resolution of 1/4° were used to obtain an overview of the ocean dynamics (Rio and Hernandez, 2004).

In addition to the hydrographic data, satellite imagery is used to detail the sea surface temperature and salinity across the Crossroad transect. Figure 3.2 illustrates both surface temperature and salinity products derived from Aquarius and SMOS. Figure 3.2 (a) shows the 7 days composite of sea surface temperature and (b) shows a temporal resolution of 10 days and a spatial resolution of 1/4° x 1/4° map of sea surface salinity. However, the 3 interdependent components of the Agulhas Current system; the Agulhas Current, Agulhas Retroflection and the Agulhas Return Current, are not well resolved and the sea surface salinity is not well defined along the coast. Therefore, for the purpose of the study these products will not be examined in detail.

Chapter 4

Results

The Agulhas Current system (ACS) is a challenging environment for the oceanography community as a result of its complex nature. Most importantly, variability along this region occurs at different scales ranging from filaments to meanders (Lutjeharms, 2006). The aim of the study is to examine both mesoscale and submesoscale variability along the Crossroad transect. The results indicate the different ocean circulation patterns observed within this dynamic region. The Agulhas Current (AC) flows along the continental shelf boundary south east of Africa from 27° to 40°S (Lutjeharms, 2006). However, the analysis provided covers the ocean domain around southern Africa from 32° to 42°S and 18° to 30°E. Above all, the region was purposefully chosen to encompass the main oceanographic features such as the AC and its return path (Agulhas Return Current), part of the Agulhas Leakage (AL), Agulhas Retroflection (AR) and Subtropical Convergence (SC) that altogether occur both up and downstream and across the transect. Therefore, this chapter will focus on the surface and subsurface measurements of sea surface height (m), temperature (°C), salinity (psu) and velocity (m/s) measured from both in situ and satellite data. For a better understanding of the ocean dynamics influencing the ACS, this sections will be divided into the 3 key questions analyzing data from 2013 to 2015. The following key questions will be addressed:

1. What basin scale features do we observe across the Crossroad transect?

2. How do observations of basin scale and mesoscale features differ when using different datasets?

3. Are there interannual similarities and differences in the basin and mesoscale variability observed along the Crossroad transect between 2013 and 2015?

4.1 What basin scale features do we observe across the Crossroad transect?

4.1.1 Altimetry and in situ measurements

2013

Represented in Figures 4.1 (a)-(c) are sea surface height maps indicating the basin scale features within the ACS. The colorbar shows positive and negative values indicating sea surface height. Overlaid on the maps along the transect are in situ data collected from the ADCP. Figure 4.1 (a) shows ranges of SSH from -2 to 2 m south of Africa measured on the 12^{th} of May 2013. The SSH ranges from 1 to 2 m illustrating the greater Agulhas system components; the AC located at approximately 36°S, AR with a southward extension located between approximately 21° and 23°E and 38° and 41°S and ARC positioned at approximately 38°S. Overlaid on the map is the surface SADCP data along the Crossroad transect as shown by the black vectors (arrows). Figure 4.1 (a) shows good correspondence between the altimetry and in situ data as indicated by the vectors. Both products indicate the intensity and direction of the AC (36°S) and ARC (38°S). This is confirmed by the length scale of the vectors with mean velocity of approximately 0.08 m/s. Encircled in blue as observed in Figure 4.1 (a) is an eddy located from 25° to 27°E and 40° to 41°S further south of the transect. Closely considering the vectors around the eddy, an anticlockwise pattern is apparent suggesting an anticyclonic eddy. The transect intersects the eastern side of the anticyclonic eddy between 26° and 28°E and 40° and 42°S. In addition, the anticyclonic eddy shows maximum SSH from approximately 0.7 to 0.9 m.

The graphical representations in Figure 4.2 (a)-(c) indicate the velocity measurements at the surface of the ocean from 35° to 42°S along the Crossroad transect with velocity measurements ranging from 0 - 2.4 m/s. The surface ADCP data exhibits the dynamic nature of the currents. Currents of the greater Agulhas system are shown in Figure 4.1 (a)-(c). Figure 4.2 highlights the surface intensified velocity signal along the transect. Areas of slow and fast currents are evident as shown on the plot indicating relative intensity currents as also seen in Figure 4.1 (a).

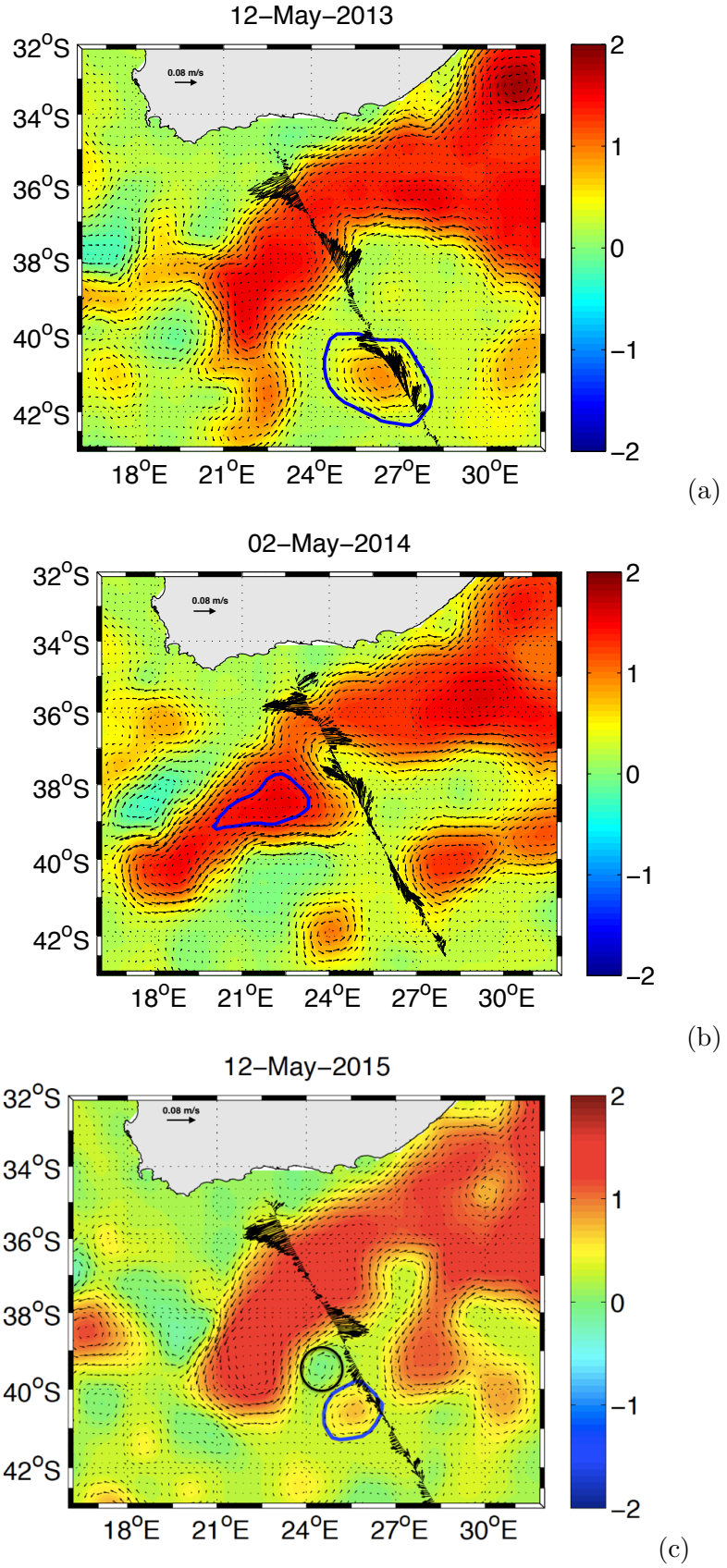

FIGURE 4.1: Maps showing SSH (m) south of Africa from 2013 to 2015. Overlaid along the Crossroad transect is the corresponding surface ADCP data as indicated by the vectors in black. The blue (black) circles indicate anticyclonic (cyclonic) eddies. The overlaid vectors show the magnitude and direction of geostrophic currents with a reference of 0.08 m/s.

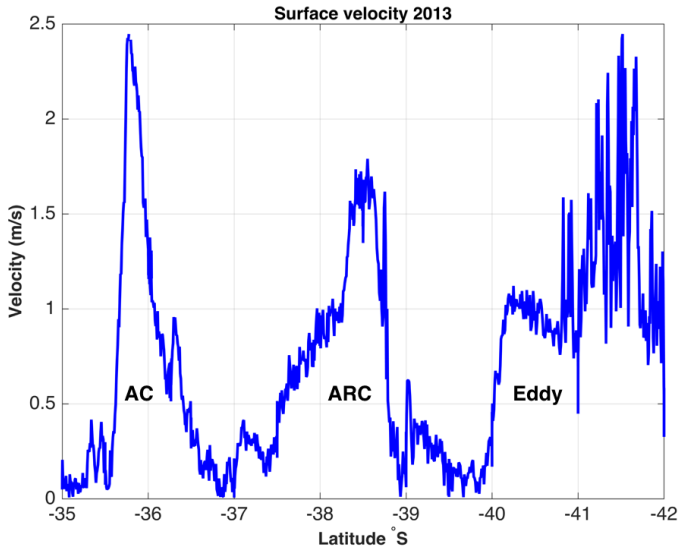

(a)

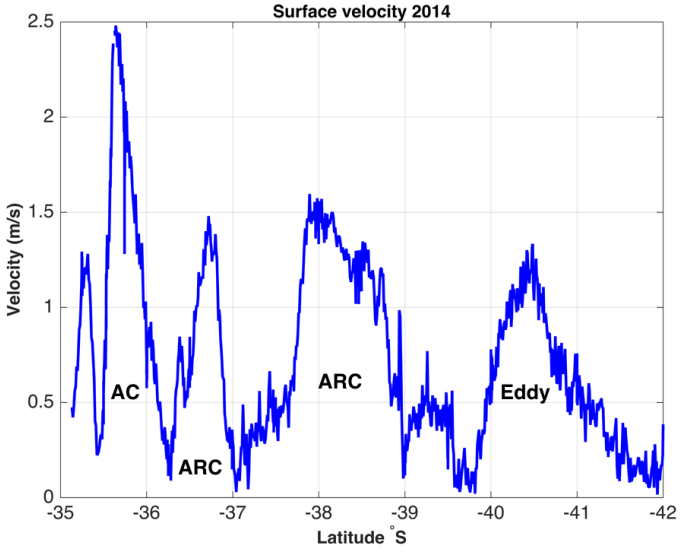

(b)

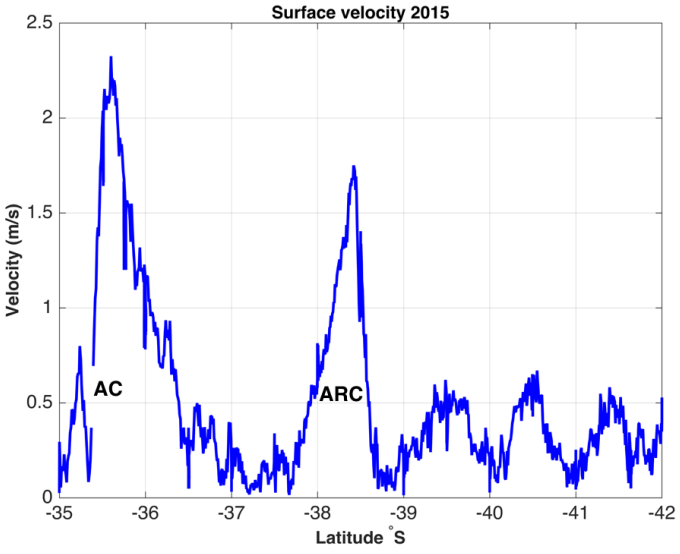

(c)

FIGURE 4.2: Velocity (m/s) plot (blue line) showing surface current intensity along the Crossroad transect obtained from SADCP data showing diferent years from 2013 to 2015. AC- Agulhas Current and ARC- Agulhas Return Current.

Figure 4.2 (a) shows the AC, ARC and an eddy. The AC is observed at 36°S with a maximum surface velocity measurement of approximately 2.4 m/s. The data highlights that the AC is a fast flowing western boundary current as concluded by Lutjeharms (2006). The high peak shows that the transect intersects the AC directly as shown in Figure 4.1 (a) suggesting the core of the current. As the transect proceeds further south from 36.8° to 37.5°S, there is a decline in surface velocity indicating areas of weak intensity of the current. An additional peak is encountered at approximately 38,5°S, slightly broader and wider compared to the AC. The peak denotes the ARC, which is different in both direction (northeast) as indicated in Figure 4.1 (a) and magnitude with minimum surface velocity of approximately 1.8 m/s. At the Agulhas Plateau (AP) (40° to 42°S), an additional ascending peak in surface velocity is observed; a mesoscale feature identified in Figure 4.1 (a) as an anticyclonic eddy. Variability is observed within the anticyclonic eddy with increasing and decreasing values (from 0.1 to 2,4 m/s) of surface velocity along the plateau. The observed eddy influences the magnitude of surface velocity with maximum measurements from 1 to 2.4 m/s.

2014

Figure 4.1 (b) shows variability of SSH values measured on the 2^{nd} May 2014 ranging from -2 to 2 m south of Africa as shown by the shading of the colorbar. The AC is located at approximately 36°S with a southwest extension apparent from approximately 17° to 18°E and 40° to 41°S. The AC forms a return flow known as the ARC, which exhibits a northward shift to approximately 37°S and continues as an eastward zonal flow towards 30°E (Ansorge, 1996). The surface SADCP data overlaid on the map similarly shows good agreement between the altimetry and in situ data as indicated by the vectors. The S shape indicates the loop of the ARC as indicated by the vectors suggesting a meandering pattern of the ARC between 37° and 40°S. The meandering of the ARC is shown by the vectors as the transect intersects the current. Locations of strong intensity (maximum vectors) indicate the positions of the AC and ARC whereas weak intensity regions are indicated by minimum vectors, suggesting weak current activity along the transect. Also important to note is the close spatial proximity between the AC and ARC between 36° and 37°S. Further south of the transect from approximately 40° to 41°S an anticyclonic eddy is observed by the pattern of the vectors. The transect intersects the western edge of the eddy. The center of the anticyclonic eddy is located at approximately 29°E and 40°S. The anticyclonic eddy observed in Figure 4.2 (a) has SSH measurements ranging from approximately 1 to 2 m.

Figure 4.2 (b) similarly indicates the AC and the ARC along the transect. The current measurements were able to identify the AC with maximum surface velocity values of down to 2.5 m/s at approximately 36°S. The ARC appears twice along the transect as a result of the meandering loop in Figure 4.1 (b) with minimum surface velocity

measurements from 1.5 to 1.7 m/s observed between 37° and 39°S. The AC is also in close proximity with the ARC as seen in Figure 4.2 (b). The 2^{nd} peak of the ARC from 37° to 39°S is relatively broader compared to the peak encountered at approximately 36.5°S. This pattern is seen similarly due to the meandering pattern in Figure 4.1 (b). At approximately 40° to 42°S along the AP, the anticyclonic eddy has minimum values of surface velocity relative to the anticyclonic eddy in Figure 4.1 (a). The variability of surface velocities between the eddy in Figure 4.2 (a) and Figure 4.2 (b) is attributed to the different positions at which the transect intersects the eddies. However, from north (35°S) to south (42°S) a consistent general pattern of increasing surface current velocity is noticed when the transect intersects an anticyclonic eddy as seen in both Figure 4.2 (a) and (b). The notable increase in surface velocity further south (along the plateau) indicates the positions at which the transect intersects the eddy. In this case (Figure 4.2 (b)), the transect intersects the western edge of the eddy at approximately 40.5°S as also seen in Figure 4.1 (b).

2015

Along the transect, Figure 4.1 (c) shows SSH south of Africa measured on the 12^{th} of May 2015. Both products illustrate good correspondence of the positions of the weak and strong currents and direction of the vectors. The vectors indicate the southwest direction of the AC, located at approximately 36°S. The ARC has a southward shift relative to Figure 4.1 (b) to approximately 39°S and the vectors illustrate an eastward direction of the current as indicated by the surface SADCP data overlaid. Along the transect at approximately 39°S a mesoscale feature identified as a cyclonic eddy (shown in blue) is observed with minimum SSH measurements of approximately -0.8 m and vectors showing a clockwise pattern. The transect intersects the eastern edge of the cyclonic eddy, encircled in black on the southern boundary of the ARC between 25° and 26°E. The center of the cyclonic eddy is noted at approximately 39,5°S and 24,2°E. At close spatial proximity to the cyclonic eddy, an anticyclonic eddy encircled in blue is also noticed as shown by maximum SSH values from 0.6 to 0.9 m and the anticlockwise pattern of the vectors. The transect similarly intersects the eastern edge of the anticyclonic eddy. The center of the anticyclonic eddy is seen at approximately 26°E and 40,5°S.

4.1.2 Which components of velocity and geostrophic velocity are observed along the Crossroad transect?

2013

Figure 4.3 illustrates the alternating (east-west) zonal (u) and (north-south) meridional (v) components of the velocity along the Crossroad transect. The u and v components

are measured from near surface to depths of down to 500 m using SADCP data whereas Figure 4.2 was limited to the surface velocity. The observed velocity throughout the vertical column indicate the intensity and direction of the current measurements from -2.5 to 2.5 m as also shown on the colorbar. For the meridional component of velocity, the AC is observed at 36°S with blue shading indicating minimum values of approximately -0.5 to -1 m/s suggesting a southward direction of the current in Figure 4.3 (a).

The positive values from 0 to 2 m/s indicate northward direction of the AC at the same latitude. At approximately 38°S northward velocity measurements of approximately 1 to 1.8 m/s are percieved as shown by the red shading suggesting the ARC position. Figure 4.3 (b) shows that the zonal component of velocity is more prominent showing an intensity of the AC at 36°S as shown by the darker shade of blue relative to the meridional component where the AC is not as clear. Altogether the meridional and zonal components suggest a strong westward and weaker southward direction of the AC. Along the coast at approximately 35°S is the bathymetry as seen by the white patches and this feature is identified as the Agulhas Bank.

Figure 4.1 (a) corroborates that the AC is directed southwest at 36°S indicating a southwest orientation of the AC from the Indian Ocean to the Atlantic Ocean. On the contrary, the northeast orientation of velocity indicates direction of the ARC at approximately 38,5°S from the Atlantic to the Indian Ocean. The anticyclonic eddy in Figure 4.1 (a) along the AP shows a northwest direction.

2014

Figure 4.4 (a) and (b) depicts the meridional and zonal components of velocity ranging from -2.5 to 2.5 m/s measured along the Crossroad transect. The vertical stripes depict the location of the currents that affect the vertical water column. Similarly, the blue shading represents the negative velocity 0 to -2.5 m/s and the red shading indicates the positive velocity 0 to 2.5 m/s. The intensity and direction of the currents differ from the coast 35° to 36°S to further offshore 37° to 42 °S. The intensity of the currents range is between -2.5 and 2.5 m/s (colorbar).

The meridional component resolves well the ARC as indicated by the red shading between 38° and 39°S in Figure 4.4 (a). Figure 4.4 (b) shows the AC and the ARC are at close proximity from near surface to 500 m. Additionally, Figure 4.4 (b) shows maximum zonal currents from 35° to 38°S. At the 36°S the AC is observed with maximum velocity measurements ranging from -2 to -2.5 m/s. The range indicates a strong southwest current. Figure 4.1 (b) corroborates the close proximity between the AC and ARC as shown by the red and blue shading at approximately 36° and 37°S. Figure 4.4 (b) also resolves well a westward direction of the AC at approximately 36°S (blue) and the eastward direction of the ARC (red) at approximately 37°S. From approximately 37°

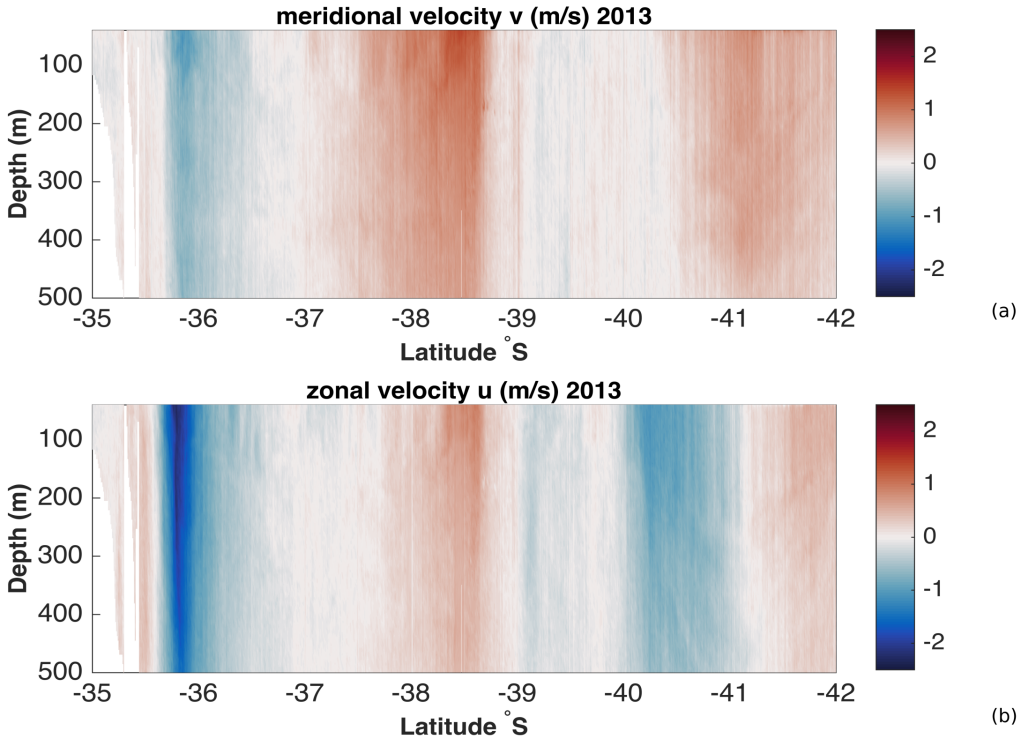

FIGURE 4.3: 2013 Vertical SADCP cross section of velocity (m/s). Positive (negative) u means eastward (westward) flow and positive (negative) v means northward (southward) flow. Vertical stripes within the velocity section are a result of alternating meridional/zonal orientation of the transect. The (u) and (v) components explain the zonal and meridional orientation of velocity (m/s).

to 39°S in Figure 4.1 (b), the transect intersects a meandering feature (S shape). Figure 4.4 (b) shows that the direction of the ARC is eastward from approximately 36.5° to 37°S with maximum velocity measurements of 1 to 1.5 m/s and westward at 38°S. The westward direction of the ARC is a result of the meandering of the current with maximum velocity measurements of -1 to -1.5 m/s. Nonetheless, the altimetry data and the in situ data exhibit good agreement of the direction of the currents as seen in both Figure 4.1 (b) and 4.4 (a) and (b).

2015

Figure 4.5 (a) and (b) depicts similarly the zonal and meridional components of velocity along the vertical column from near surface to 500 m. The zonal component shows a stronger vertical shear variability with maximum velocity measurements from -2,5 to 2,5 m/s. Figure 4.5 (a) shows the north-south components where positive (0 to 2,5 m/s) is north and negative (0 to -2,5 m/s) is south. Figure 4.5 (a) does not resolve well the intensity of the currents relative to Figure 4.5 (b), which shows a strong signal of velocity throughout the vertical column. In addition, Figure 4.5 (a) shows less variability in terms of current activity from near surface to depth of 500 m as shown by the faded

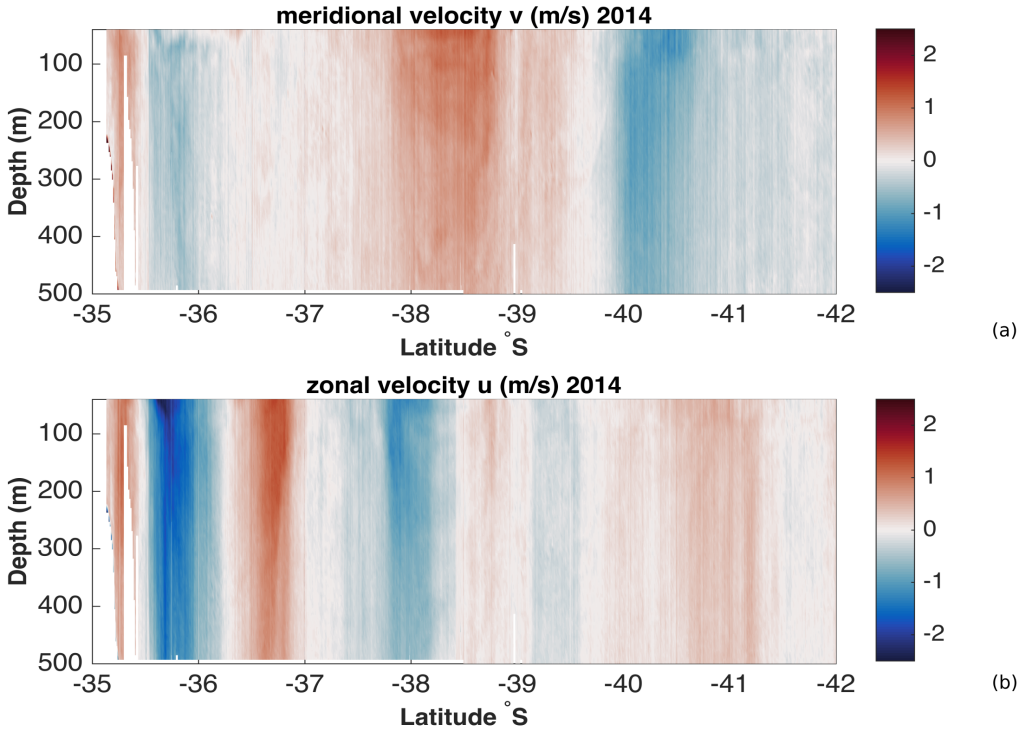

FIGURE 4.4: 2014 Vertical SADCP cross section of velocity (m/s). Positive (negative) u means eastward (westward) flow and positive (negative) v means northward (southward) flow. Vertical stripes within the velocity section are a result of alternating meridional/zonal orientation of the transect. The (u) and (v) components explain the zonal and meridional orientation of velocity (m/s).

blue and red shading. The north south components are not well resolved compared to the zonal component of velocity in Figure 4.5 (b). The altimetry data in Figure 4.1 (c) shows that the AC at 36°S is directed westward and the ARC at 38°S eastward, hence less north-south velocity are resolved in Figure 4.5 (a) with minimum velocity measurements from approximately 0 to 0.5 m/s and 0 to -0.5 m/s (This means that there are weaker meridional velocities as opposed to weak meridional velocities not being resolved essentially). In Figure 4.5 (b) the negative velocity measurements from -1 m/s to 2,4 m/s (blue) is strongly illustrated close to the coast from 35,5° to 36°S indicating surface intensified velocity signal of the AC. Figure 4.5 (b) shows that the AC has a westward direction in Figure 4.1 (c). At about 38°S the positive velocity (red) measurements from 1 to 1.7 m/s illustrate the ARC with an apparent eastward direction. Figure 4.5 (b) shows a further southward shift of the ARC to approximately 38°S in Figure 4.1 (c) relative to the position of the ARC at 37°S in Figure 4.1 (b). This also suggests that there is a good correspondence between the observed altimetry and in situ data.

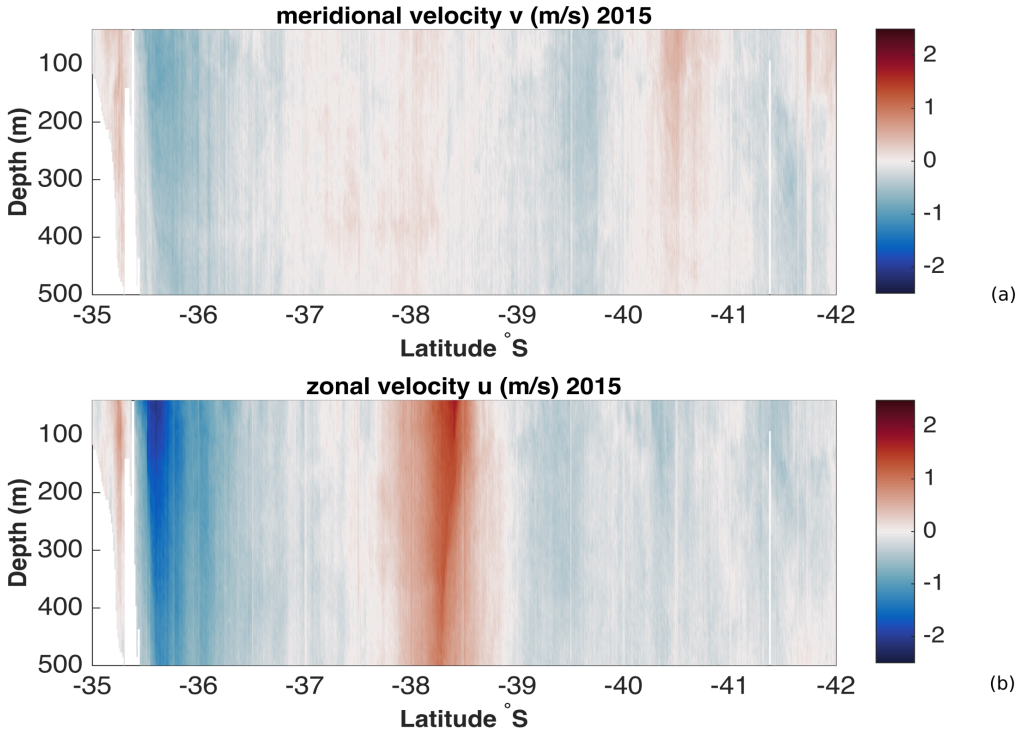

FIGURE 4.5: 2015 Vertical SADCP cross section of velocity (m/s). Positive (negative) u means eastward (westward) flow and positive (negative) v means northward (southward) flow. Vertical stripes within the velocity section are a result of alternating meridional/zonal orientation of the transect. The (u) and (v) components explain the zonal and meridional orientation of velocity (m/s).

4.1.3 Geostrophic velocity

Figure 4.6 (a)-(c) illustrates the dynamics of the Crossroad transect, based on geostrophic velocities obtained from hydrographic data such as temperature, salinity and density from 2013 to 2015. The maximum geostrophic velocity measurements from 0 to 1 m/s and minimum values 0 to -1 m/s indicate the flow of the current due to the balance between pressure gradient and Coriolis force known as geostrophic balance ($(\frac{1}{\rho})(\frac{\partial p}{\partial x}) = fv$). The geostrophic velocity ranges from -1 to 1 m/s indicating varying strength of the flow of the currents. The AC has geostrophic velocity measurements from -0.2 to 0.8 m/s, while the ARC has values of down to 0.2 to 0.6 m/s proceeding further offshore as shown by the velocity contours. Positive (negative) values indicate the direction of the flow. Considering the compass direction NW and NE are positive and SW and SE are negative. The data reveals a strong SW flow of the AC and NE ARC in Figure 4.6 (a)-(c). The blue (red) shading represents the AC (ARC) (see colorbar) and the contour interval is 0.2 m/s (see velocity contours).

2013

In Figure 4.6 (a) the flow of the AC is seen at 36°S down to approximately 20 to 30 km close to the coast. The AC extends further from near surface to depths of down to 1400 m. The geostrophic currents reproduce well the southwest flow of the AC. The close proximity of the velocity contours indicate the strength of the AC. Notable differences between the AC and ARC are shown; the ARC flow is observed at approximately 38°S proceeding further offshore, extending to depths of down to 1200 m. In addition, the ARC also exhibits a broader V shaped pattern flow towards the sea floor. The presence of eddy activity in this region is well resolved at the AP as illustrated by the 0.2 m/s geostrophic velocity contour. The sharp point of the V shape well resolves position of the core of the AC at 36°S and the ARC at 38°S as in Figure 4.6 (a). The extend of the AC further towards 1400 m relative to the ARC suggests an influence of a strong bottom current.

2014

In Figure 4.6 (b) the flow of the AC is similarly closer inshore and extends to depths of approximately 1250 m. The AC is noted in close proximity to the ARC. At 37°S the ARC is spotted with a depth of approximately 640 m and a NE direction. At 38°S is the ARC with a different direction (SW) as a result of the meandering pattern seen in the altimetry data in Figure 4.1 (b) with a depth of approximately 700 m. A relatively quiescent flow along the AP is shown as documented by the -0.1 m/s geostrophic velocity contour flowing to a depth of approximately 690 m. The geostrophic flow of the AC exhibits minimum geostrophic velocities from -0.1 to -0.6 m/s while the ARC is noticed with maximum geostrophic velocities of 0.1 and 0.4 m/s from approximately 37° to 39°S.

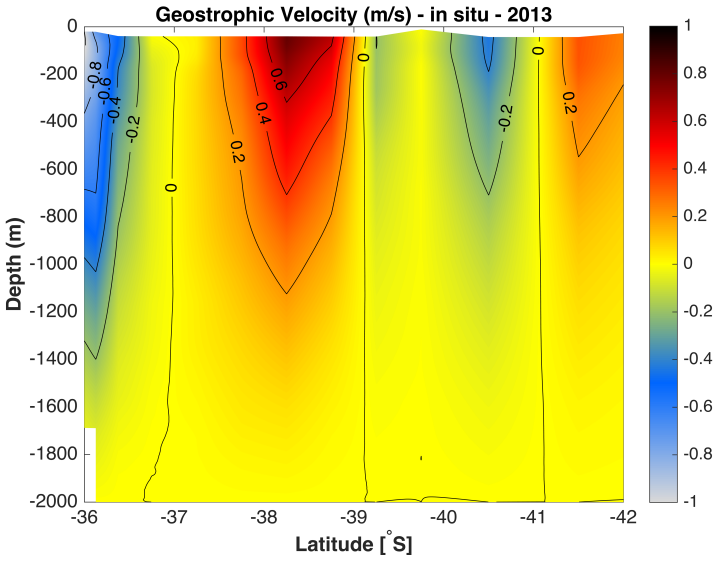

(a)

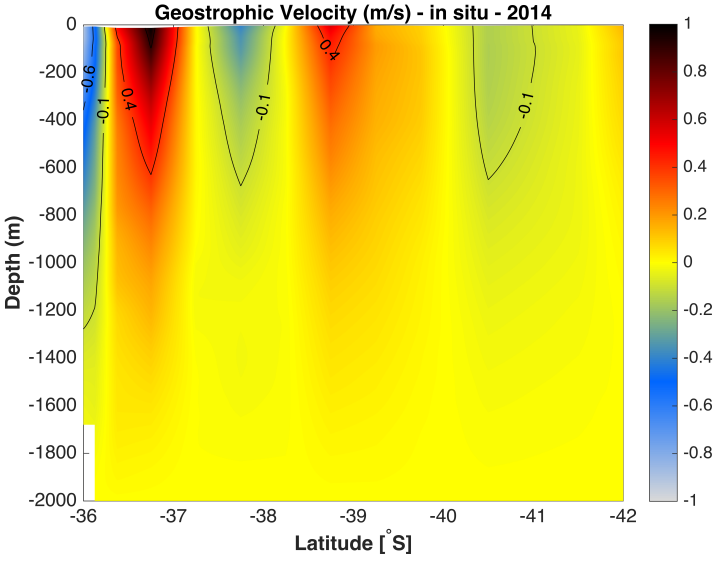

(b)

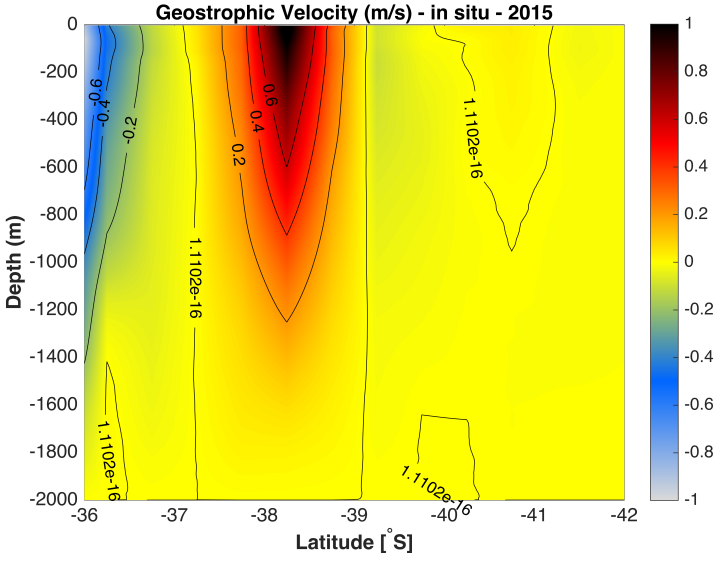

(c)

FIGURE 4.6: Meridional vertical profiles through the top 2000 m showing geostrophic velocity along the Crossroad transect. The contour interval is 0.2 m/s. Considering the compass direction NW and NE are positive and SW and SE are negative.

2015

In Figure 4.6 (c) the flow of the AC is deep extending further to approximately 1400 m (see the blue shading). The AC exhibits maximum flow from -0.2 to -0.6 m/s as shown by the geostrophic velocity contours. Between 36° and 37°S from 1400 to 2000 m minimum geostrophic flows are noticed, which suggests an influence of bottom currents. A strong return flow is also observed with flows from approximately 0.2 to 0.6 m/s (see the red shading) with a strong NE direction. The V shaped pattern of the ARC is similarly demonstrated between 38° and 39°S. The geostrophic velocities vary considerably with ranges from -1 to 1 m/s and the variability thereof will be discussed in detail in the next chapter.

4.1.4 Water mass property distribution

The water mass property distribution along the Crossroad transect is presented in Figure 4.7 (a)-(f). Both the temperature and salinity sections were computed from near surface to a depth of 2000 m to highlight the salient features along the transect and water mass distribution. The variability in salinity distribution observed is qualitatively similar to the temperature distribution; as the temperature decreases towards the sea floor the salinity also changes relatively as illustrated by the different water masses.

2013

The isotherms illustrated by the black lines indicate temperature differences from near surface to a depth of approximately 1600 m in Figure 4.7 (a). The temperature measurement as shown by the isotherms range from 4° to 22°C. At about 35.5 °S the Agulhas Bank depicts a strong temperature gradient with temperatures down to 20°C. Sloping isotherms go as deep as 1400 m along the continental shelf. Also evident at approximately 35.5°S is an uplift pattern of isotherms, which suggest and upwelling of cold water from 1300 m as shown by the 4°C isotherm towards the surface at approximately 200 m as shown by the 10°C isotherm. At 36°S the AC is indicated by an increase in temperature along the surface with temperature values of down to 22°C. The temperature increases at the core of the AC and decreases further south. From 36.25° to 38°S a warm pool of water is observed with temperature values from 14° to 20°C and a depth range from near surface to approximately 400 m and shown by the isotherms and red and yellow colorbar. Further offshore at approximately 39°S the ARC is distinguished as shown by the deepening of the isotherms. The ARC is characterized by cool temperatures relative to the AC with a maximum temperature of 14°C while the AC has a maximum temperature of 22°C. Therefore, as observed at 39°S the temperature for the ARC range from 4° to 14°C.

Figure 4.7 (d) shows the meridional vertical section of salinity ranging from 34° to 36 °S as shown by the colorbar. Along the Agulhas Bank, isohalines show an uplift of water from 900 m to 200 m suggesting an upwelling of lower salinity water characterized with minimum salinity values from 34.6 to 34.8 psu. The cold of low saline water contains properties of SICW, which will be discussed further in the next section. At 36°S the AC is characterized with maximum salinity from 34.8 to 35.6 psu. Between 36.25° and 37.5°S the warm pool is characterized with salinity content from 34.6 to 35 psu with an apparent difference in water mass properties from near surface to depths of 1700 m. Maximum salinity ranges from 35 to 35.6 psu from near surface to approximately 650 m. Low saline waters are distinguished from 800 to 1700 m with minimum salinity values from 34.4 to 34.8 psu. At 39°S the ARC is seen with minimum salinity values from 34.4 to 35 psu suggesting that the ARC has relatively lower salinity compared to the AC.

2014

Figure 4.7 (b) shows the vertical meridional section of temperature along the Crossroad transect. Along the Agulhas Bank at approximately 35.5°S a strong temperature gradient is observed as shown by the isotherms with minimum temperature values from 4° to 10°C observed between depths of 400 and 1650 m and maximum temperatures from 14° to 22°C from near surface to approximately 100 m. The AC is observed at 36°S as shown by the deepening of the isotherms with maximum temperature values from 4 to 22°C. The warm loop of water is observed between 36.25° and 36.5°S as also shown by the stratified pattern of isotherms. At 37°S the ARC is seen further offshore and as a result of the meandering loop as seen in Figure 4.1 (b). The ARC is also noticed at approximately 39°S with relatively cooler temperature values from 4° to 20°C. At approximately 36°S, the AC is relatively deeper reaching a maximum depth of 1400 m while the ARC is observed at 1100 m at approximately 39°S.

The upwelling of lower salinity water is also noticed at the Agulhas Bank with salinity values of 34.4 to 34.8 psu. The salinity signature in Figure 4.7 (e) show minimum variability with salinity ranging from 34 to 36 psu. Deepening of the isohalines indicate the AC at 36°S with maximum salinity content from 35 to 35.6 psu. The influence of the meandering pattern is also apparent within the salinity signature further offshore from 37° to 39°S. The ARC at 39°S exhibits relatively similarity range of salinity signature with the AC possibly due to the close proximity between the currents in Figure 4.7 (e). In addition to the meandering pattern in Figure 4.1 (b) the depth of the AC and ARC is also variable with the effect of the AC reaching a maximum depth of 850 m and the ARC at approximately 700 m as remarked by the 34.6 psu salinity isohaline. This suggests that the effect of the AC is deeper than the ARC.

2015

Figure 4.7 (c) shows the vertical section of temperature along the Crossroad transect. Close to the coast at approximately 35.5°S relatively cool waters are observed from 200 m to 1000 m with minimum temperature values from 4° to 10 °C. At 36°S the AC is observed with maximum temperatures from 4° to 22°C. The warm pool of water from 36.5° to 37.5°S reaches a maximum depth of approximately 1000 m with apparent horizontal stratified isotherms suggesting also the shallowing of the isotherms. Further offshore east of the warm pool from 38°S, the ARC is observed with relatively minimum temperatures from 4° to 14°C. The 22°C isotherm is only observed from 35.5° to 36.3°S from near surface to approximately 50 m. Following Emery (2001), four water masses are recognized in the upper 1500 m in Figure 4.7 (c) and (f).

Below the maximum salinity values with a range between 35 and 35.6 psu from near surface to a depth of approximately 1000 m, minimum salinity values ranging from 34.2 to 34.8 psu are observed. According to Emery (2001), these surface maximum salinity properties are identified as the Tropical Surface Water (TSW) and Subtropical Surface Water (STSW). At intermediate level from approximately 1500 m the (Antarctic Intermediate Water) AAIW are observed as characterized by lower salinity water properties. The salinity minimum as shown by the 34.4 psu isohaline at approximately 37°S indicates more pronounced AAIW reaching a depth of approximately 1800 m while at 39°S shallower AAIW are observed with a depth of approximately 950 m. At approximately 39°S a minimum isohaline of 34.2 psu is observed. Furthermore, the AAIW are illustrated by low saline and cold waters and will be discussed further in the next section.

Water mass properties illusrated by vertical profiles and T/S diagrams along the Crossroad Transect

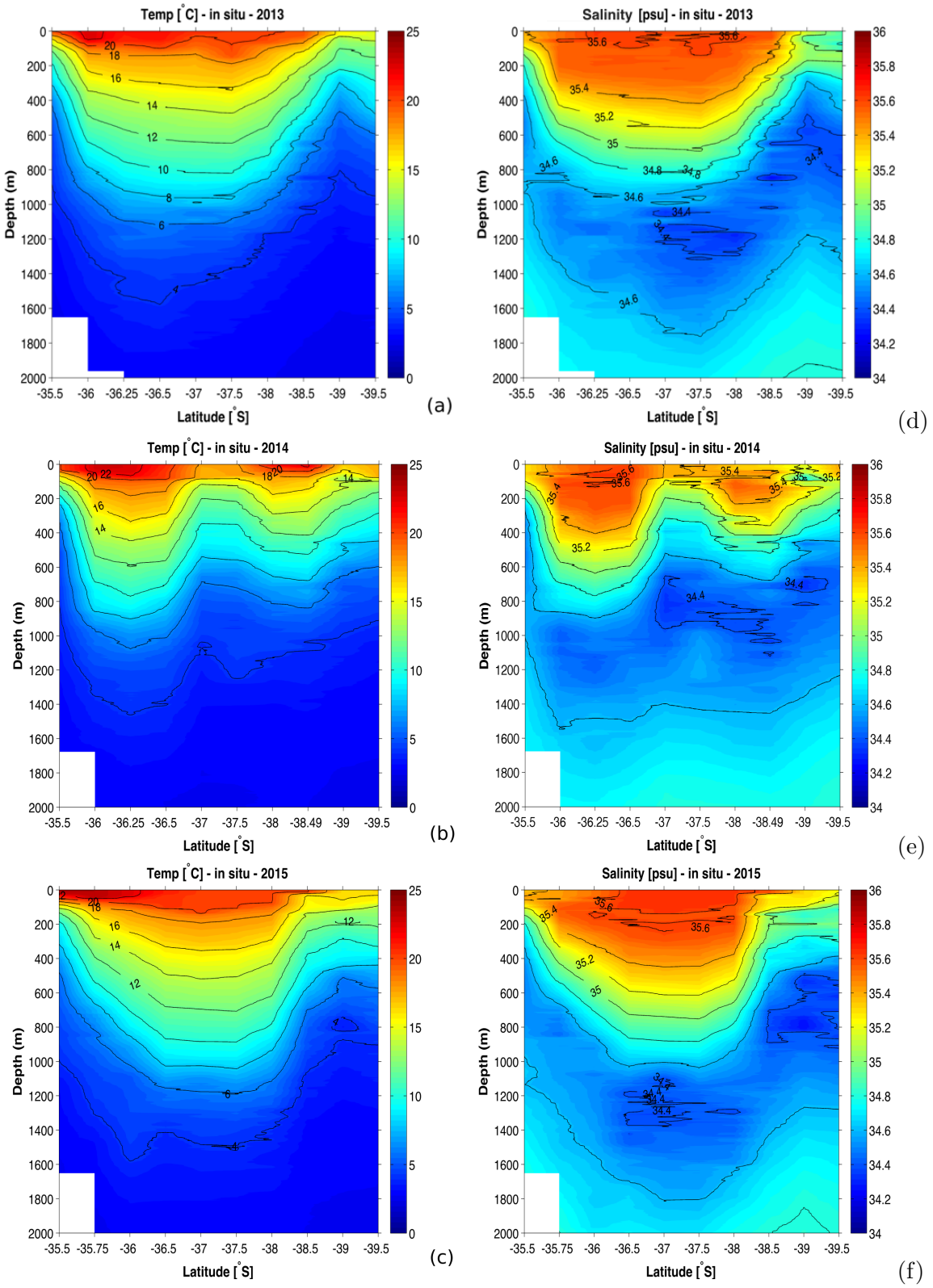

FIGURE 4.7: Meridional vertical profiles through the top 2000 m of temperature and salinity along the Crossroad transect. The contour interval of temperature is 2°C and salinity is 0.1 psu.

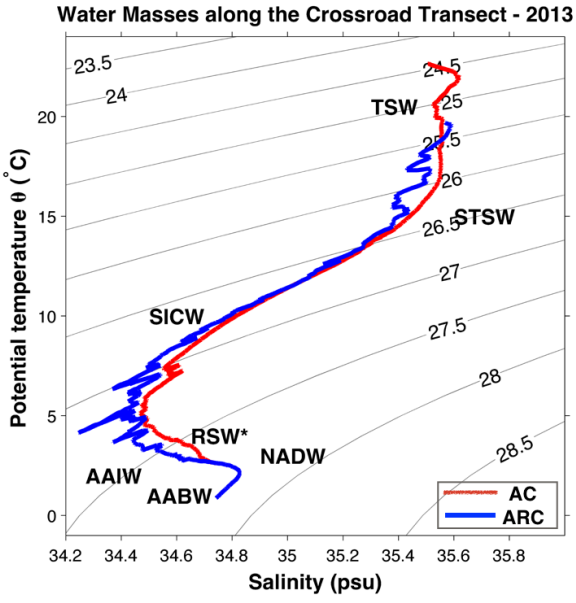

FIGURE 4.8: T/S diagrams for water mass properties extracted along Crossroad transect. The Red line indicates the Agulhas Current and blue line the Agulhas Return Current. The following water masses are represented: TSW, STSW, SICW, RSW, AAIW, NADW and AABW. The asterisk represents remnants of RSW.

Salinity as a function of potential temperature diagrams are presented in Figure 4.8 (a)-(c) extracted from the Crossroad transect at different positions of both the AC and ARC from 2013 to 2015. It is worth noting that water mass modification and an influence of ocean density are among one of the factors that result from salinity variation along the transect (Nyadjro and Subrahmanyam, 2015). Essentially, the T/S diagrams are used to infer on different water types; water masses and their spatial distribution. The T/S diagrams show that the water mass properties of the AC and ARC differ from surface to deep layers. Given the variability of the AC and ARC as observed in the velocity profiles (Figure 4.2) and meridional sections (Figure 4.7), the water masses in the T/S diagrams exhibit similar variability at surface and subsurface layers. The water masses identified are therefore classified according to their distribution in the water column. Observed from Figure 4.8 (a)-(c) are the surface and thermocline waters; the Tropical Surface Waters (STW), Subtropical Surface Waters (STSW) and South Indian Central Waters (SICW) from 0 to 500 m, Antarctic Intermediate Waters (AAIW) and Red Sea Water (RSW) from 500 to 1500 m and deep and abyssal waters, North Atlantic Deep Waters (NADW) and the AABW from 1500 m to the ocean floor. The y-axis shows potential temperature and salinity is represented by the x-axis as illustrated by Figure 4.8 (a)-(c). The density in the background ranges from 23.5 to 28.5 kg/m^3. This section provides a clear distinction of water masses and the distribution thereof using their salinity and temperature properties.

2013

Figure 4.8 (a) shows water masses of the AC in red and ARC in blue. The water masses observed from near surface to 500 m are characterized with lower salinity from 35.4 to 35.5 psu and temperature from 14° to 22°C, owing to excess warming and precipitation over evaporation near the equator (Toole and Warren 1993; de Ruijter et al., 1999). These waters represent the TSW as categorized by Emery (2001) and intrude the AC waters through the Mozambique Channel (de Ruitjer., et al 2002). Subsequently, the salinity maximum water masses identified as the STSW are observed with salinity of down to 35.6 psu and also form as a result of high evaporation within the subtropical gyre. The surface water masses; TSW and STSW exhibit neutral densities from 24.5 to 26.6 kg/m^3. The AC and ARC exhibit similar SICW with cool and lower salinity water properties of neutral density between 26.5 and 27 kg/m^3. At intermediate depths below the thermocline Figure 4.7 (a) exhibits lower salinity AAIW and remnants of saline RSW. The AAIW illustrate minimum salinity values from 34.3 to 34.5 psu and the RSW modifies the salinity content to about 34.7 psu saline waters. According to Beal., et al (2006), these RSW sink as a result of excess evaporation within the Red Sea basin and due to its high volume of approximately 0.5 Sv (Sv= 10^6 m^{-3} s^{-1}) remnants of these waters are traced across the equator and southern Indian Ocean and enters the AC via the Mozambique Channel (Beal et al., 2000). The bottom and deep water

observed in Figure 4.8 (a) include the AABW and the NADW, which potentially flow northward within the Agulhas Undercurrent (Beal and Bryden, 1997).

2014

Comparing the water properties of the AC and ARC Figure 4.8 (b) shows distinctive differences between the two currents notably at surface, intermediate, bottom and deep layers. At surface layers TSW along the AC are clearly resolved with a maximum temperature of approximately 22°C and salinity from 35.4 to 34.5 psu. The ARC water properties resolve well the STSW relative to the TSW. The STSW of both the AC and ARC differ slightly with the salinity content; the ARC exhibits maximum salinity of 35.2 psu while the ARC shows relatively more saline STWS with maximum of 35.6 psu. The SICW are also relatively different between the two currents and the difference is possibly due to the meandering of the ARC. The major difference of the water mass properties between the AC and ARC is observed at the intermediate and bottom layers with high neutral densities from 27.5 to 28.5 kg/m^3.

2015

The surface water masses; TSW and STSW similarly exhibit neutral densities from 24.5 to 26.5 kg/m^3 as shown by the isopycnals. In Figure 4.8 (c) the STSW of the AC are more saline relative to the AC waters as also observed in Figure 4.8 (b). Figure 4.8 (a)-(c) altogether show an upwelling of cool salinity minimum SICW. Figure 4.8 (c) shows both the AC and ARC intersect the 27 kg/m^3 isopycnal and show similar water properties. At intermediate layers the AAIW and remnants of the RSW are displayed with minimum salinity content of down to 34.4 psu and salinity maximum of approximately 34.65 psu. The NADW have a salinity maximum of 34.8 psu propagating southward with maximum depth from 1500 to 2000 m and AABW exhibit minimum salinity of approximately 34.7 psu at bottom layers.

4.2 How do observations of basin scale and mesoscale features differ when using different datasets?

4.2.1 Altimetry data

Considering the SSH maps (Figure 4.1 (a)-(c)), a noticeable variation in the position of the AC and ARC is observed. The spatial variation is observed in terms of the shifting of the currents as a result of their dynamic nature. The ARC in 2013 is observed at 38°S, with a relatively further spatial proximity to the AC. In 2014 the counter current (ARC) is at close spatial proximity to the AC at approximately 37°S and proceeds further southward in 2015 at approximately 39°S. Interesting to note is that the position of the AC remains stable as its core is observed at approximately 36°S from 2013 to 2015 with less or minimal variation. In addition to the spatial variation is the direction of the currents, with the AC also consistently flowing relatively southwest as displayed in Figure 4.1 (a)-(c). Conversely, the ARC exhibits change in direction from 2013 to 2015 though its structure resembles that of the AC (Boebel et al., 2003). In 2013, the ARC exhibits a north east direction at approximately 38°S, a parallel direction with the AC eastward at 37°S and northwest between 38° and 39°S in 2014 due to the meander and likewise eastward at approximately 39°S in 2015. The superposition of the resulting surface SADCP data indicates variability in the velocity intensity from the start (35°S) to the end (42°S) of the transect. The mesoscale features; anticyclones and cyclone observed along the transect also differ spatially in terms of size and position from 2013 to 2015 and are possibly shed from the AC and ARC (Boebel et al., 2003). Also worth noting is that the transect successfully intersects both the AC and the ARC on all 3 occasions (from 2013 to 2015) as per motivation of the study behind the Crossroad transect.

The AC and ARC both encounter different oceanographic processes and variability (Rouault, 2011). The AC flows close to the shore with minimum variability observed along the Agulhas Bank (Bryden et al., 2005; Gründlingh, 1983). Further offshore (south) the current exhibits numerous meanders, fronts and eddies. At a spatial scale, variability observed along the Crossroad transect exhibits different water properties of the AC relative to the ARC. Compared to temperature, salinity measurements have been inadequate and altogether these measurements are essential for understanding of oceanographic processes including air sea interactions (Nyadjro and Subrahmanyam, 2015). To better understand the spatiotemporal variability along the Crossroad transect, a graphical representation of sea surface salinity derived from TSG and CTD is displayed in Figure 4.9 (a)-(c) from 2013 to 2015.

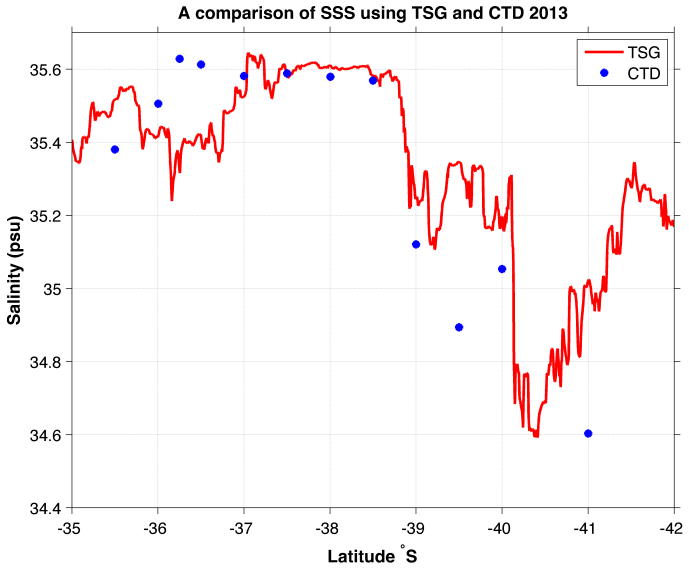

(a)

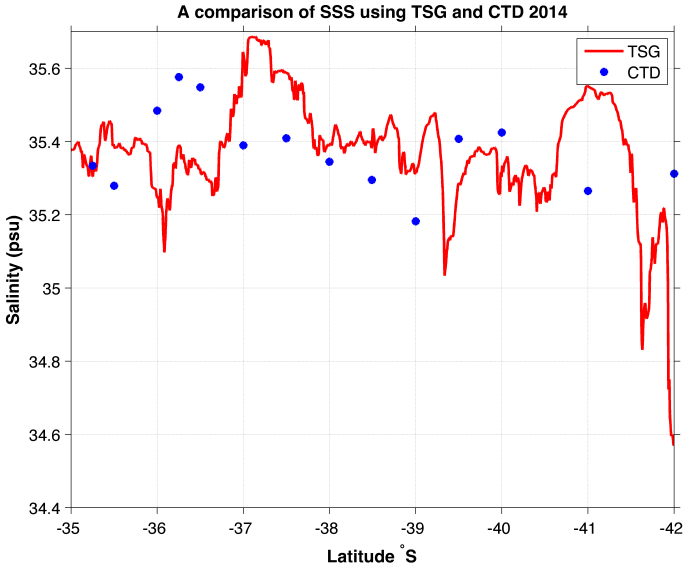

(b)

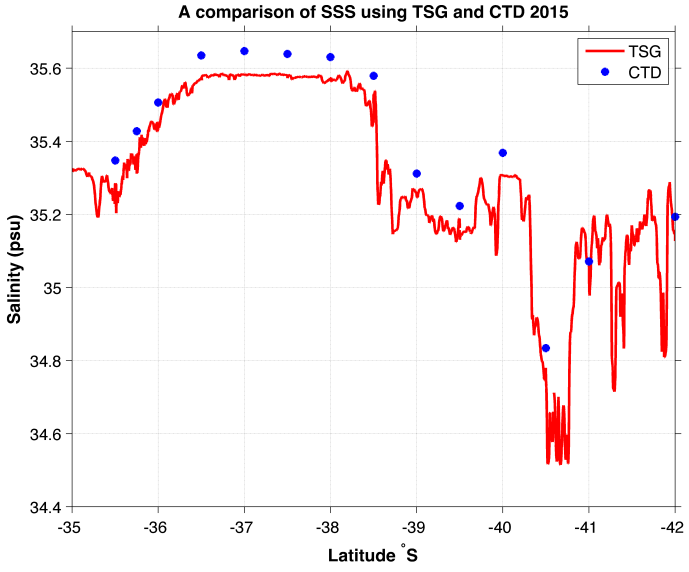

(c)

FIGURE 4.9: A comparison of sea surface salinity using TSG and CTD datasets along the Crossroad transect. The blue dots (red line) represent the CTD (TSG) data.

4.2.2 Sea surface salinity (SSS) measurements from Thermosalinograph (TSG) data

A comparison of high resolution TSG and low resolution CTD data are demonstrated in Figure 4.9. A variant nature of the Agulhas system is observed from 35° to 42°S considering the salinity signature in the region. The general trend exhibits a fluctuation of salinity values along the surface. A clear distinction of the differences between the CTD and TSG data depicts a nonlinear pattern along the Crossroad transect. The CTD data shows data at specific station positions in blue dots while the TSG data shows continued measurements of surface salinity data with a red line. The CTD and TSG measurements in Figure 4.9 are obtained from an iso-surface within a depth range of between 4 and 8 m as the CTD does not sample exactly at the surface of the ocean. As a result of the high spatio-temporal resolution, more processes are captured using TSG data as compared to the low resolution CTD measurements hence the ability to observe different salinity measurements between the two datasets as seen in Figure 4.9 (a)-(c). It is worth noticing the presence of meanders and shear edge pertubations at the inshore edge of the Agulhas Current that potentially induces localized upwelling along the Agulhas Bank (Largier et al., 1992).

2013

The pattern illustrated by the blue dots shows variability of SSS along the transect. The variability thereof is displayed through consistent increase and decrease in SSS. At 35°S (AB), an increase in SSS is observed from approximately 35.4 to 35.6 psu. The maximum SSS measurements exceeding 35.5 psu indicate the AC. Further south from 37° to 39°S of the transect a slight decrease in SSS is observed with a constant variation of SSS measurements ranging from 35.56 to 35.58 psu. A sharp decrease in SSS is also observed with minimum SSS measurements between 34.90 and 35.1 psu also suggesting the ARC. At 41°S a minimum salinity measurement of 34.6 psu is observed. The TSG SSS measurements similarly exhibit variability along the transect as shown by the red line. Evident between 35° and 36°S is an increase and decrease in SSS with measurements from approximately 34.4 to 35.56 psu. From 36° to 37°S there is an increase in SSS with measurements from 35.25 to 35.6 psu also indicating properties of the AC and capturing processes and events of warming and cooling as a result of the high resolution. Between 37° and 39°S the SSS measurements from the CTD and TSG are in good correspondence with constant measurements from 35.56 to 35.58 psu. TSG measurements further south from 39°S exhibit a sharp decrease in SSS from 35.6 to 35.2 psu. Relative to the CTD, TSG measurements also indicate more saline water properties between 39° and 40°S with measurements ranging from 35.5 to 35.3 psu. Another sharp decrease in SSS is observed at 40°S to minimum SSS of approximately 34.6 psu and in addition at the same latitude an increase is observed with SSS measurements from 34.6 to a maximum

of 35.35 psu. A sudden increase in SSS is observed at 40°S consequently due to the anticyclonic eddy as identified in Figure 4.1 (a). The CTD data points however fail to capture the signal of the anticyclonic eddy.

2014

Considering Figure 4.9 (b) a comparison between SSS using CTD and TSG is shown, with blue dots similarly indicating CTD stations and red line indicating the TSG measurements. From the AB at approximately 35°S an increase of SSS is observed from 35.25 to 35.58 psu. Between 37° and 39°S a decreasing pattern of SSS is seen with minimum SSS measurements from 35.40 to 35.19 psu. Between 39° and 42°S again variability is noticed with SSS measurements observed ranging between approximately 35.2 and 35.4 psu. Overall the CTD SSS measurements show an increase and decrease pattern along the transect. On the other hand, the TSG measurements similarly exhibit variability spatially along the transect. Between 35° and 36°S the red line illustrates SSS measurements fluctuating from approximately 35.10 to 35.40 psu suggesting the AC in Figure 4.1 (b). An increasing pattern percieved from 36° to 37°S with maximum SSS measurements of approximately 35.65 psu suggesting the ARC. Between 37° and 39°S the ARC is shown in Figure 4.1 (b) and a fluctuating pattern with SSS decreasing from 35.65 to 35.40 psu from 37° to 38°S and additionally showing a constant decreasing signal with minimum SSS of 35.4 psu between 38° and 39°S. Furthermore, at the AP a dome feature is distinguished, which is identified as an anticyclonic eddy in Figure 4.1 (b). The anticyclonic eddy exhibits an increase in SSS measurements with maximum of 34.53 psu, which is relatively higher compared to the CTD data point measured at that latitude.

2015

Figure 4.9 (c) likewise shows the comparison of SSS between CTD and TSG measurements along the Crossroad transect. Evident along the transect is a consistent correspondence between the two datasets. Between 35° and 36°S an increasing pattern is observed with SSS measurements from approximately 35.20 to 35.52 psu. Both the CTD and TSG SSS measurements show a constant signal with less SSS variation between 37° and 38°S. The CTD SSS measurements are relatively higher with constant value of approximately 35.64 psu and TSG exhibits minimum value of approximately 35.59 psu. A decrease in SSS is observed from 38,5°S with fluctuations ranging from 35.35 to 35.56 psu. Furthermore, another decrease in SSS is observed from 40°S and variation is evident further towards 42°S due to the anticyclone and cyclone eddies observed as seen in Figure 4.1 (c). Comparison of Figure 4.9 (a)-(c) shows an inconsistent agreement between the SSS measurements collected from CTD and TSG. There are visible discrepancies between the SSS measurements from both datasets. In both Figure 4.9 (a) and

(c) considering SSS measurements from approximately 37° to 39°S, there is less shear variability along the transect as a result of the warm pool that is observed between the AC and ARC as seen in Figure 4.1 (a) and (c). Figure 4.9 (b) however, shows that there is more shear variability as a result of the close proximity of the AC and the ARC. Altogether from 2013 to 2015 the CTD dataset does not provide convincing evidence of mesoscale activity along the transect and the interannual variability will be discussed further in the next chapter.

4.2.3 Temperature and salinity measurements from Thermosalinograph

The Thermosalinograph system was run for the duration of the voyage for the collection of data along the Crossroad transect. An examination into the ships trajectory allowed an evaluation of the upper water properties such as temperature and salinity; their distribution throughout the ocean. Documented graphically in Figure 4.10 (a)-(c), the distribution of the open ocean is apparent with the salinity signature and temperature outlined.

2013

Figure 4.10 (a) shows predominantly the main features along the transect as annotated (see the shear variability along the transect). A notable change in water properties is mostly observed where the transect passes the basic oceanographic features. Both the AC, ARC and an eddy have an in influence on the water properties. The AC has the highest temperature measurements. Between 36°S and 37°S the highest temperature is approximately 24°C representing the AC. Between 38°S and 39°S the ARC exhibits decrease in surface temperature with values from 15° to 20°C. Between 39° and 40°S, likewise a notable decrease in surface temperature is seen. The general pattern indicates that the warmer the current, the lesser the salinity. The salinity variation along the transect also indicates warming and cooling events of the currents. The AC illustrates less saline water properties relative to the ARC. Between 35° and 37°S minimum salinity measurements down to 35.4 psu are observed, while further south from 37° to 38°S there is a constant salinity signal suggesting mixing of water and also showing maximum ARC salinity of approximately 35.6 psu. It is worth noting the influence of the eddy from approximately 40° to 42°S on the water properties along the transect. Along the AP an increase in both hydrographic measurements are shown by the rise in amplitude. The surface temperature of the anticyclonic eddy observed has an increase of approximately 3°C increasing from 13° to 16°C. Similarly, the salinity ehxibits an increase of approximately 0.8 psu with a maximum saline value of approximately 35.4 psu.

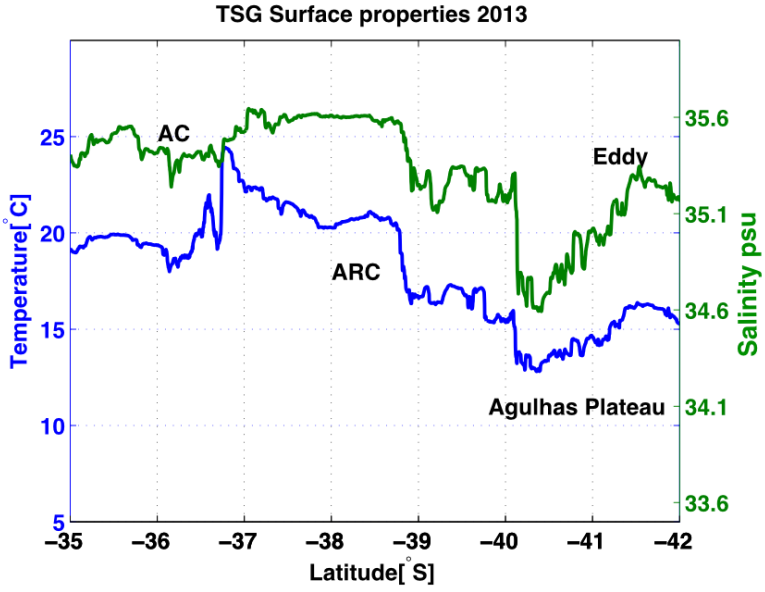

(a)

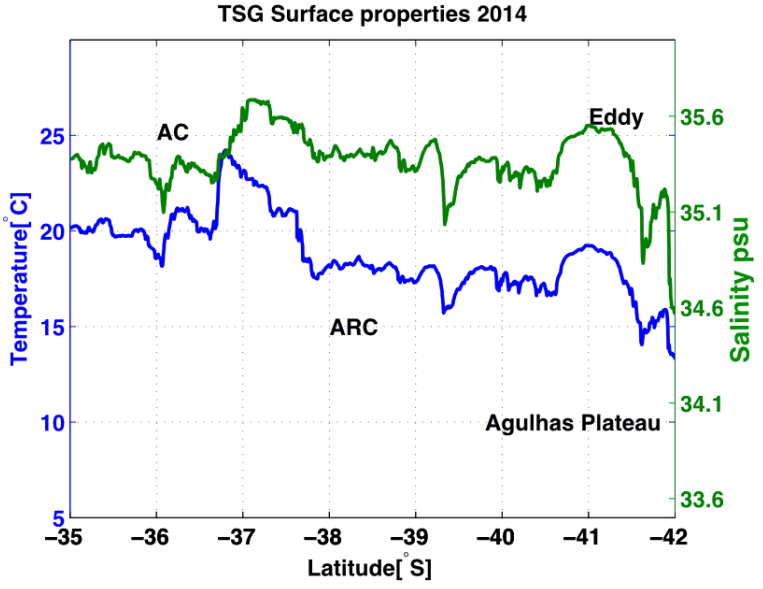

(b)

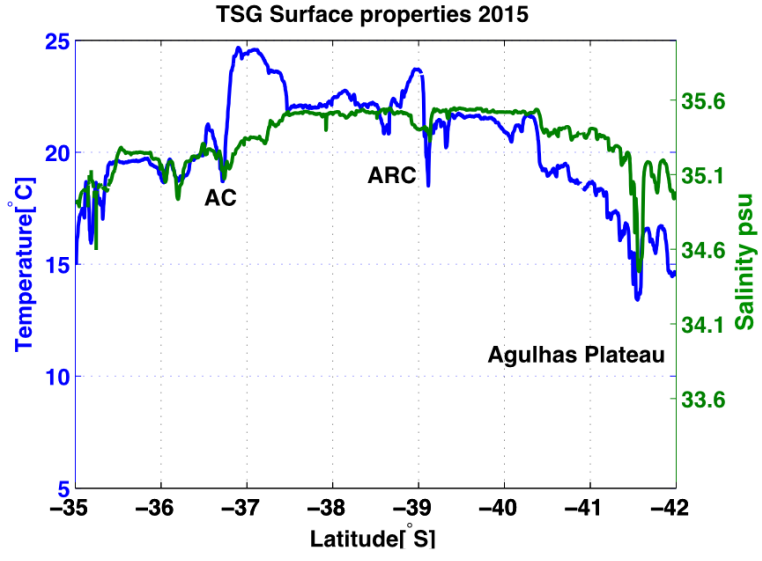

(c)

FIGURE 4.10: Sea surface temperature and salinity obtained from Thermosalinograph dataset. The blue (green) line indicates temperature (salinity) and the following annotations are observed AC- Agulhas Current and ARC- Agulhas Return Current.

2014

Figure 4.10 (b) similarly illustrates varying hydrographic properties and how they are influenced by small and large scale features along the Crossroad transect. As expected along the AC, between 35° and 36°S there is a notable increase in temperature from 18° to 22°C. Subsequently, a strong gradient is observed with a sharp peak at approximately 37°S suggesting the location point of the ARC. The TSG measurements also illustrate a decreasing pattern of temperature from 37° towards 39°S with surface temperatures reducing from as high as 24° to 17°C possibly representing subtropical surface water mass properties. Further south along the AP an anticyclonic eddy is observed with temperatures between approximately 16° and 19°C as indicated by the rise in amplitude. Similarly, the salinity variation of the AC exhibits less content relative to the ARC. The minimum surface salinity measurement of AC is approximately 35.1 psu while the maximum ARC measurements are down to 35.7 psu. The salinity of the ARC is therefore relatively higher due to the cool temperatures. As a result of the close spatial proximity between the AC and ARC the salinity signal captures relatively similar water properties. The eddy is characterized by similarly increasing saline properties with a maximum of approximately 35.50 psu.

2015

Figure 4.10 (c), in addition also constitutes of substantial variability of hydrographic properties along the transect. The characteristics of the surface waters are distinguishable between the AC and ARC. In the surface temperature range between 15° and 22°C, the AC is observed from 35° to 37°S. A transition between the AC and ARC is separated by a strong vertical gradient as observed at 37°S. Between 37° and 38°S there is a notable increase in surface temperature from 21° to 24,5 °C. Also notable between 37,5° and 39°S is a constant temperature measurement of approximately 22°C representing mixing along the spatial proximity between the AC and ARC as also seen in Figure 4.1 (c). At 39°S the ARC is observed with maximum surface temperature of approximately 23°C suggesting an influence of warm tropical surface water. Changes in salinity measurements are also evident in 2015 and have a potential to influence ocean density and modify properties of various water masses. Although the variation in surface salinity along the transect is not as high as temperature, salinity continues to provide a strong salinity signal along the transect.

4.3 Are there interannual similarities and differences in the basin and mesoscale features observed along the Crossroad transect?

Dynamical properties such as temperature and salinity along the surface are observed.In Figure 4.11, the interdependent components of the Agulhas system (AC and ARC) are highlighted with the AP annotated between 40° and 42°S. Sea surface temperature signal along the Crossroad transect varies with temperature ranging from approximately 13.5° to 24.5°C. An increment in surface temperature is shown from the AC from 35° to 37°S. A decline in temperature is illustrated from 37° to 39°S. In both 2013 and 2014, along the AP there is a distinct increase in temperature values. The increase in surface temperatures along the plateau was attained in response to the eddies as seen with dome like features. In 2015 a decreasing trend is noticed along the AP. Therefore, variability in temperature observed along the sea surface is possibly due to the north and south movements of fronts, and as the transect intersects either cyclonic or anticyclonic eddies.

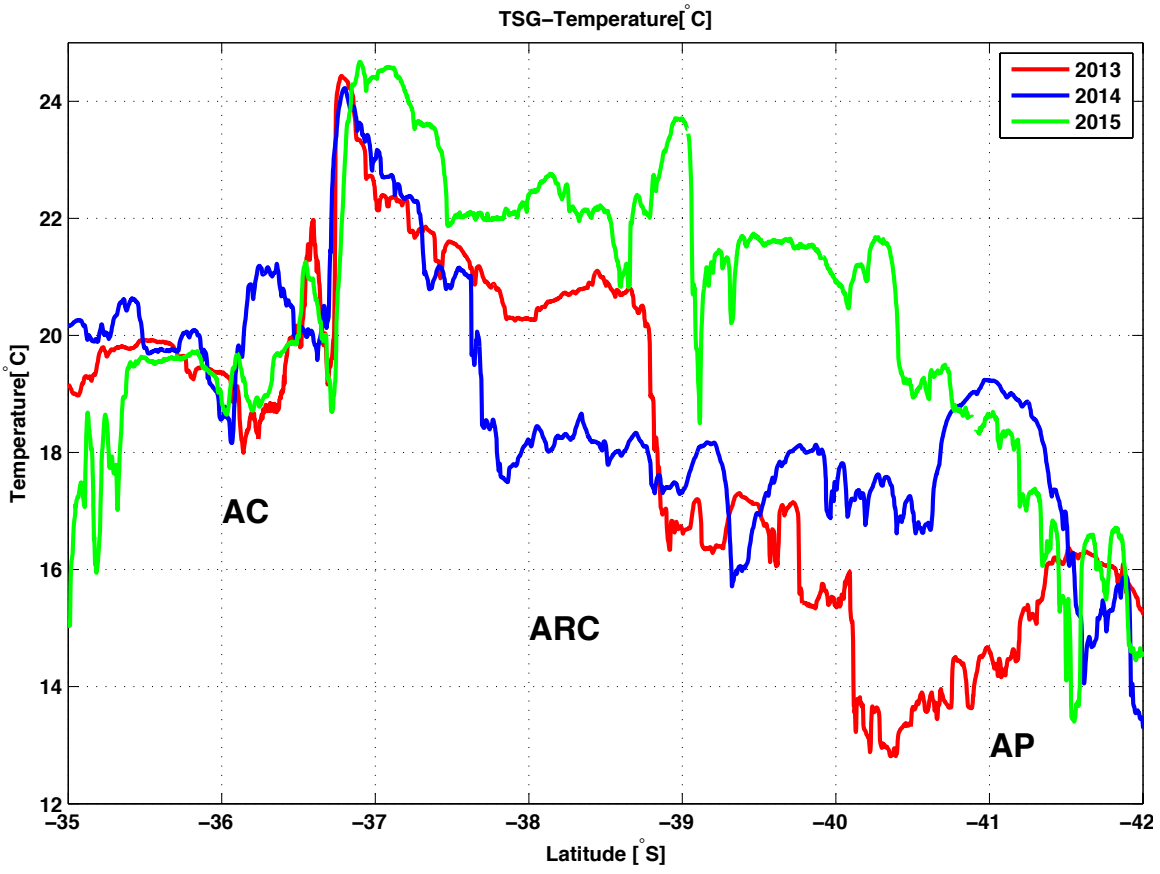

FIGURE 4.11: Surface temperature measurements collected from Thermosalinograph dataset along the Crossroad transect. The following annotations are observed; AC- Agulhas Current, ARC- Agulhas Return Current and AP- Agulhas Plateau.

4.3.1 What are the similarities in surface temperature along the Crossroad transect?

The interannual variability across the Agulhas system plays a defining role in determining its behavior. To assess the interannual evolution of the sea surface state along the Crossroad transect, data collected from the TSG is considered. The interannual variations observed in Figure 4.11 represent short term interannual variability from 2013 to 2015. The graphical representation of sea surface temperature along the transect are shown by different lines; 2013 illustrates properties in red, while 2014 is represented by the blue line and the green line indicates the 2015 surface temperatures as shown in the legend. Between 35° and 37°S a warming pattern, suggests the transition to warmer waters as observed with surface temperature increasing from 15° to 25 °C and a strong temperature gradient observed at approximately 36,5 °S. A general pattern of decreasing temperatures is similarly observed from 37° to 39°S. A constant pattern of surface temperature is shown between 38° and 39°S. In 2013 and 2014 the surface temperature exhibit increasing maximum temperature along the AP. However, notable is the decreasing surface temperature at the same latitude (39° to 40°S) in 2015. From 2013 to 2015 the submesoscale features are evident, with a horizontal length scale of approximately 1 to 10 km. These features are apparent throughout the transect indicating a region of high variability. They are identified as filaments and fronts and exist within the mesoscale features as observed in Figure 4.11 (see the shear variability along the AP). Along with the mesoscale features these patterns exhibit spatial interannual variability along the transect from 2013 to 2015.

4.3.2 What are the differences in surface salinity along the Crossroad transect?

The differences in surface temperature observed along the transect are mostly documented along the ARC from approximately 37° to 39°S. In 2013 the surface temperature observed decrease from 24,5°C to 16,3°C. In 2014 a decrease in surface temperature observed is from 24,5°C to 17,5°C. Lastly, 2015 exhibits surface temperature decreasing from 24.5° to 21°C suggesting altogether that the ARC is relatively warmer in 2015 as shown by maximum temperature compared to the 2013 and 2014. Also evident along the AP are the differences not only in surface temperature, but in the size of the mesoscale features observed. The anticyclonic eddy observed in 2013 has relatively minimum surface temperature ranging from 13° to 16°C. Also notable is the size of the eddy with a large spatial proximity of more than 150 km. In 2014 maximum surface temperature ranging from 16° to 19°C are observed along the anticyclonic eddy with a relatively small spatial proximity of approximately 100 km. In 2015 however, the surface temperature illustrates a decreasing pattern from approximately 19° to 13,5°C.

4.3.3 Sea surface salinity signature along the Crossroad transect

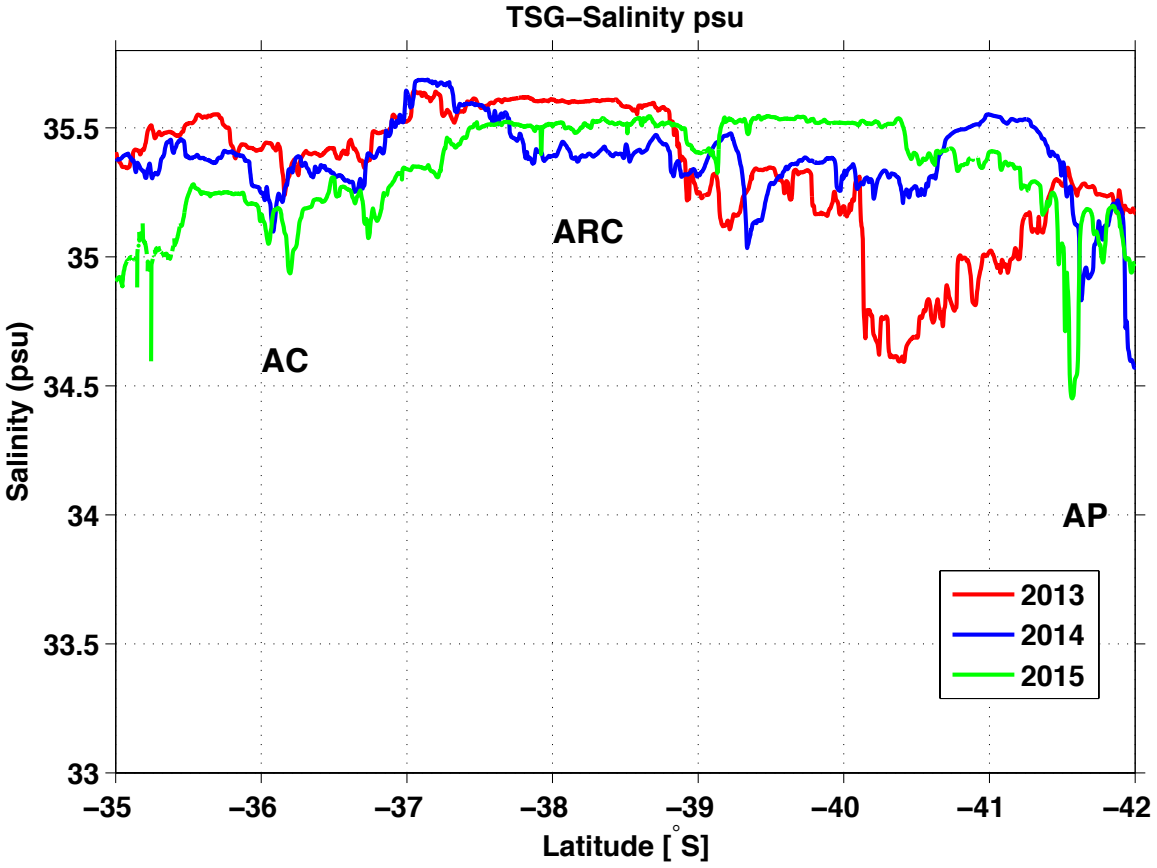

FIGURE 4.12: Surface salinity measurements collected from Thermosalinograph dataset along the Crossroad transect. The following annotations are observed; AC- Agulhas Current, ARC- Agulhas Return Current and AP-Agulhas Plateau.

The salinity signature observed along the Crossroad transect is similarly subject to variability although more consequential relative to temperature, due to its conservative property. The salinity measurements along the transect are less varied. A notable distinction as seen in Figure 4.12 is the difference between the AC and ARC. The ARC exhibits more saline surface waters relative to the AC. The difference is possibly due to temperature differences between the currents. Anticyclonic eddies in the southern hemisphere are characterized by warm temperature, therefore as a result of the presence of the eddy observed along the AP warmer surface waters are observed ranging from 13° to 19°C. Along the AP, in the years 2013 and 2014 the salinity content is relatively higher than in 2015 where a declining pattern is observed. The eddy distinguished in the year 2013 is less saline and more broad compared to the eddy observed in 2014 (see Figure 4.12) . In 2015 the spike observed at approximately 35.2°S represents an incorrect data. Such data can be corrected using software such as QTSG. The large dome shaped patterns represent mesoscale features and the small shear variability denotes submesoscale features. Essentially, the mesoscale variability is observed through the salinity and temperature observed along the transect. The graphical representations

observed in both Figure 4.11 and Figure 4.12 document different spatial and temporal differences interannually from 2013 to 2015.

Chapter 5

Discussion

The basin scale circulation around the Crossroad transect is encompassed of complex ocean features and is well known for its dynamic nature. The study will also closely examine mesoscale variability across the Crossroad transct. In examining the basin scale and mesoscale variability across the Crossroad transect, the following key questions will be addressed:

1. What basin scale circulation features do we observe across the Crossroad transect?

2. How do observations of basin scale and mesoscale features differ when using different datasets?

3. Are there interannual similarities and differences in the basin scale and mesoscale features observed along the Crossroad transect between 2013 and 2015?

5.1 What basin scale circulation features do we observe along the Crossroad transect?

The Agulhas Current System is an oceanic system consisting of different characteristics that fundamentally allows for a broad observation of both spatial and temporal variability for the benefit of scientific communities. In an attempt to understand and analyze the basin scale circulation across the transect, the following features are evident, namely the main interdependent components such as the AC and ARC. The core of features are also highlighted using altimetry data, providing an ideal opportunity to study their path and variability. The northward and southward shifting of the ARC observed in the years 2014 and 2015 as shown Figure 4.1 (b) and (c), contribute to the overall poleward shifting of the Agulhas Current System (Beal et al., 2011). The AC and ARC also demonstrate a change in latitudinal position from 2013 to 2015. In 2013, the AC (36°S) was approximately 270 km apart from the ARC(38°S). In 2014 a northward shift

is observed with the ARC (37°S) at close proximity, approximately 70 km to the AC. Similar to 2013, the ARC is observed further south at approximately 39°S. Previous studies show that the impact of the shifting current plays an important role in strengthening the AMOC (Beal et al., 2011; Yang et al., 2016). The variability in the strength of the Agulhas Current has also been observed with maximum velocity exceeding 2.5 m/s, as initially shown by previous research studies (Lutjeharms, 2006; Morris et al., 2017). The mesoscale features, such as eddies and meanders are also identified. It is worth noting that although the Crossroad transect is situated at the same position annually, it may intersect different positions of these mesoscale features as a result of their transient nature and ocean dynamics of the ACS. Furthermore, these ocean features influence the oceanic conditions south of Africa, hence the need to understand their nature. The mesoscale variability occurs as linear planetary waves and as non linear vortices, which potentially transport momentum, heat, mass and chemical constituents of seawater, therefore contributing to the general ocean circulation, large scale water mass distributions and ocean biology (Robinson, 1983). The mesoscale activity that occurs along the Crossroad transect is also important because the eddies found in this region carry water masses that have different water properties from their surrounding and enhance mixing as they dissipate (Gamoyo et al., 2017). Previous knowledge has shown how the intensification of these features has an influence downstream. Although the Agulhas Retroflection and leakage do not form part of the Crossroad transect, considering the basin scale features these components may provide a better overview of the potential impacts on the southern african climate system. Moreover, previous studies have also highlighted the thermohaline contributions of the leakage to the AMOC through the Indo- Atlantic exchange (Beal et al., 2011; Gordon 1986; Van Sibille et al., 2009).

The water masses presented in this study exhibit substantial ocean circulation variability based on observational data. Ubfortunately the water mass properties cannot be concluded from the altimetry data, hence the need for in situ data to understand better the variation in water mass distribution along the Crossroad transect. However, the results indicate from both the altimetry and in situ products a similar general pattern in the varying position of the AC and ARC along with the associated mesoscale features. The altimetry data has successfully demonstrated the variant nature of the ACS along with its associated surface properties. Figure 4.1 (a)-(c) altogether display an overview of the basic salient features across the Crossroad transect and sea surface height is used as a proxy to evaluate the mesoscale variability in the region. Having identified the basin scale features along the transect, it is moreover important to understand both spatial and temporal variability. Considering the SSH diagrams as displayed in Figure 4.1 (a)-(c), it is notable that submesoscale features are not well resolved or identified on the ocean surface as a result of their horizontal length size (1 km). Thus, the challenge in accurately measuring these features with low resolution satellites (McWilliams, 2006). Nonetheless, different oceanic observations as seen from Figure 4.1 to Figure 4.8 resolve well the salient oceanographic features along the transect using different data products

from surface to subsurface layers. Therefore, the main objective, which is to illustrate the importance of each product in highlighting the processes associated with the ACS. Altogether, the altimetry and in situ products exhibit the spatial and temporal variability of the ACS. The altimetry data however, has demonstrated more variation across the transect, enabling a broader context of the basin scale features associated with the ACS and providing more understanding of the WBC and its trajectory south of Africa.

In identifying the basin scale features along the transect, variation in velocity, geostrophic velocity, temperature and salinity at both surface and subsurface are well resolved. A combination of these variables contribute to the understanding of different oceanic observations including small and large scale ocean circulation and climate change around South Africa and globally. Interesting to note is the surface velocity variation observed in Figure 4.2. In comparison to Figure 4.2 (a) and (c), Figure 4.2 (b) illustrates an abundance in surface velocity measurements. The cause of the variation in relation to the different years is to date not well known, however different processes including upstream events resulting from the sources of the Agulhas Current may have a contribution to the ocean variability in this region. It is also important to have different visual representations of velocity along the Crossroad transect in order to understand both surface and subsurface variations, including velocity influenced by the balance between pressure gradient and Coriolis force (geostrophic velocity). The magnitude of surface velocity of the AC and ARC have been quantified as seen in Figure 4.2 (a)-(c). Different components of surface velocity have been observed including both the zonal and meridional velocity, which altogether illustrate the current intensity and velocity structure throughout the vertical column from near surface to 500 m. Similarly, the geostrophic velocity observed in Figure 4.6 reproduce well the basin scale features along the Crossroad transect. However, relative to the velocity measurements observed in both Figure 4.2 to Figure 4.5, Figure 4.6 illustrates geostrophic velocity from near surface to a maximum depth of approximately 2000 m. Overall, the velocity measurements complement each other and highlight the main features of the ACS. To ireterate, the altimetry data highlights the main components of the ACS without demonstrating the complexity in the system and therefore allows some insight on its global ocean circulation role. In addition, although the domain has been reduced to show the main features of the ACS it is clear that the system has an influence from its upstream sources, such as the South Equaitorial Current, East Madagascar Current and Mozambique Channel.

5.2 How do observations of basin scale and mesoscale features differ when using different datasets?

Previous knowledge demonstrates the importance of understanding different oceanographic scales and the role of the ACS (Bela et al., 2011). For example, Lutjeharms

(2006) conveyed the Agulgas Current as a WBC primarily driven by large scale pattern of wind stress. Observations of basin scale and mesoscale features, differ in size from one dataset to another and are similar in terms of illustrating the predominant structure of the ACS. These exclude the Agulhas Retroflection and leakage as the focus of the study is based along the Crossroad transect. Although the observations show a similar predominant structure of the ACS, different interpretations depending on the type of dataset and variable analyzed are observed. These include the altimetry data in Figure 4.1, which shows the structure of the ACS through sea surface elevation (SSH). The variation of SSH from 2013 to 2015 is observed and a good correspondence between the SSH and surface ADCP data is highlighted. The mesoscale features are also observed in Figure 4.1 and altogether the anticyclonic and cyclonic features differ in size and as transect intersects these features at different positions each year. Figure 4.1 also highlights the importance of variability through the trajectery of the Agulhas Current, allowing migration of water from the Indian Ocean to the Atlantic Ocean on a spatial scale, which is not well defined on other in situ products. Nonetheless, the in situ datasets compliment the altimetry data as more understanding on water mass distribution is provided. The velocity plot shown in Figure 4.2 resolves well both basin and mesoscale structures and both features are quantified. The magnitude of surface velocity (0-2.5 m/s) is outlined and maximum surface velocities are observed between 35° and 37°S. Similarly high variation in surface velocity is observed in 2014 relative to 2013 and 2015. Highlighted from Figure 4.3 to 4.5 are vertical sections of velocity measured from SADCP data. Relative to Figure 4.2 these diagrams exhibit both the zonal and meridional components of velocity. However, the mesoscale features are not well resolved in comparison to the surface velocity observed in Figure 4.2. The opposite occurs in Figure 4.7 where geostrophic velocity measurements are observed. The mesoscale features are well resolved in Figure 4.7 (a) and (b). In comparison to Figure 4.9, Figure 4.10 illustrates both SSS and SST along the Crossroad transect, providing an overview of the surface variation of both basin and mesoscale features. Figure 4.9, through the use of CTD data also highlights the gaps missing when comparing different resolution datasets. SWOT mission envisions providing 2D SSH at a spatial resolution ten times higher relative to conventional altimeters, although with a lower temporal resolution from 10 to 20 days. In doing so the aim is to provide snapshots of small scale variability within the swaths, assuming the spatial resolution is sufficient enough to resolve small scale features. In defining variability on both spatial and temporal scales along the Crossroad transect, it is important to note that over 99% of the kinetic energy of ocean currents is associated with variable mesoscale features (Munk, 2000). The kinetic energy of these mesoscale variability, which has scales of 10 to 100 km and 10 to 100 days, is more than an order of magnitude greater relative to the kinetic energy over most of the oceans (Wyritki et al., 1979; Richardson, 1983). In addition, Munk (2000), put forward that at the opposite end of the general ocean circulation, the microscale exists (from millimeters to centimeters) where energy is irreversibly converted to heat

(Ferrari and Wunsch, 2009). Therefore, the scale at which these energy processes occur should not be underestimated because they are small.

In essence, the submesoscale motions have a potential impact on mesoscale variability providing a much richer variety of dynamical regime (Klein et al., 2015). These mesoscale and submesoscale variability and its associated eddy fluxes and vertical exchange play an important role in ocean circulation dynamics and physical biological coupling (Klein et al., 2015). Variability along the Crossroad transect was defined by the variant mesoscale and submesoscale features. Using altimetry data (Figure 4.1 (a)-(c)) the mesoscale features identified include cyclonic and anticyclonic eddies and the meandering of the ARC. These mesoscale features are different in terms of their form, structure and are transient in nature. The submesoscale on the other hand is identified as flow structures with length scale range of between 0.1 and 10 km (McWilliams, 2006). These features are not observed using altimetry data (SSH) due to the limited low spatial resolution (1/4° x 1/4°). A detailed study of these features will also improve our knowledge on the mean variability of the ACS (Rouault, 2011). The in situ data collected using TSG clearly exhibits these features along the surface as shown in Figures 4.11 and 4.12.

Temperature is a thermodynamic property of a fluid and it changes as a result of processes such as heating, cooling and diffusion. Salinity, on the other hand varies due to an addition or withdrawal of low saline water, thus altering the dilution of salts (Tally et al., 2011). Considering air-sea interactions, solar heating and wind are proven the main drivers of evaporation from the surface of the ocean to the atmosphere leading to an increment of salinity in a defined volume of sea water (Yu, 2011). The AC also produces high latent heat fluxes and transports moisture to the atmosphere (Rouault et al., 2003b). The salinity signature thus provides an indication of the hydrological balance between the atmosphere and ocean, and most importantly can be used for the reduction of uncertainties in surface lower salinity water flux estimates in the ocean rain gauge regime (Köhler, 2015). Consequently, variations of sea surface salinity are an expression of changes in low saline water transports (Köhler, 2015). Altogether temperature and salinity variations as seen in Figure 4.8 have a great influence on the density of seawater and the entire ocean circulation across the Crossroad transect. In addition, the salinity variations are a consequence of a changing ocean circulation as a result of vertical mixing processes and associated salt exchanges between surface and sub surface layers. It is worth noting also that the hydrographic variation along the transect is essential as it provides a better if not broad view of the vertical structure, surface and subsurface circulation as a result of the available observational data presented.

Yu (2011), describes that salinity distribution at the surface changes in response to the spatial and temporal variations in the net surface freshwater flux. Another important factor that influences salinity variation and distribution is horizontal advection by ocean currents (Köhler, 2015). Salinity has historically been known as one of the most under sampled properties resulting in an elusive detailed knowledge of the long term ocean

salinity variability. Considering Figure 4.7, the variation along the Crossroad transect is also documented east of the south coast by the intense southward flow of the AC and the variant meandering of the zonal ARC. The change in position of the ARC also indicates the dynamic nature of the current. On the vertical cross sections of temperature and salinity the effect of the AC and ARC on the water column changes from one year to the other, which suggests an influence of the currents on the water properties as seen in Figure 4.7 (a)-(f). Upwelling of cold waters are observed close to the coast as depicted by the distribution of isotherms in Figure 4.7 (a)-(c). This uplift introduces cold nutrient rich SICW (Figure 4.8) waters on the shelf (Agulhas Bank). Understanding the different water properties along this region is important as it supports approximately two-thirds of the Cape Anchovy spawner population. In addition, it is home for a majority of diverse fish species (Hutchings, 1994; Roy et al., 2007) and has potential ecological and economic benefits for South Africa. The SICW have temperature and salinity range of 8° to 13°C; 34.8 to 35 psu, which coincides with the SICW as classified by (Emery, 2001). Variations in water properties are well resolved as seen in Figure 4.7 (a)-(f), which are attributed to the nature and distribution of water masses. In addition, upwelling observed along the AB results in cooling of surface waters, which is effectively substantial for the growth, decay and instability of ocean fronts and filaments (Shillington, 2006). Despite the temperature and salinity changes from one year to another along the surface, different water masses similarly exhibit the tendency of varying hydrographic properties at deep layers. Furthermore it is worth noting that from Figure 4.1-4.8, the submesoscale features are not well resolved relative to Figure 4.9-4.12.

5.3 Are there interannual similarities and differences in the basin and mesoscale features observed along the Crossroad transect between 2013 and 2015?

Results altogether indicate a pattern of increasing variability across the Crossroad transect, which occurs also as a result of the influence of the subtropical gyre and other upstream events relating to sources of the ACS (Shillington, 2006; Lutjeharms, 2006). Altimetry data, as seen in Figure 4.1 (a) and (b), indicates that the years 2013 and 2014 are predominantly dominated by mesoscale features. The transect intersects different mesoscale features in different years. Also interesting to note is the meandering pattern of the current in the year 2014, which is indicated by an S shape. The nature of this mesoscale feature can be attributed to the dynamic trajectory of the AC and possible varying current intensity from 2013 to 2014. With numerous differences in mesoscale features observed along the transect, the area continuously remains largely variable, dynamic and complex. Furthermore, the transect intersects both the basin scale features including the mesoscale features as illustrated in Figure 4.1 (a)-(c). Also to note is that the transect intersects mostly the anticyclonic features relative to the cyclonic features. The distinction between the three years is evident with the years 2013 and 2014 (Figure 4.2 (a) and (b)) indicating eddy features further south along the AP. The intensity of velocity along the plateau (from 40° to 42°S) ranges from 0 to 0.7 m/s in 2015 (Figure 4.2 (c)) where the transect intersects the eastern edge of cyclonic and anticyclonic eddies. The maximum surface velocity measurements in mesoscale activity are observed in 2013 and 2014 with a velocity range from 0 to 2.4 m/s in 2013 and 0 to 1.3 m/s in 2014 as seen along the AP. In addition, Figure 4.2 (a)-(c) both highlight the basin scale and mesoscale features with high variability in velocity. The direction of the currents varies from one year to another as documented from Figures 4.3 to 4.5.

Considering the vertical cross sections in Figures 4.3 to 4.5, the intensity of the currents vary both zonally and meridionally from near surface to depths of approximately 500 m. In addition, these figures suggest that the intensity of velocity decreases from north to south (35° to 42°S) according to the position of the currents. Therefore, a notable difference in the direction of the currents is observed from Figures 4.3 to 4.5 where the meridional and zonal components of velocity are displayed. The general trend in the morphology or structure of the AC and ARC is captured with the AC´s trajectory flowing south west of the east coast of southern Africa and the ARC remaining zonal with varying meandering patterns as seen in Figure 4.1 (a-c). Similarly, the flow of the AC and ARC is well resolved using geostrophic velocities as observed in Figure 4.6 (a-c). The high velocity shear including the meandering fronts motivate mixing of different water mass properties in the Agulhas system region (Emery, 2001).

The circulation of the ocean is a result of the balance between different forces. And the frictional force is the most important force in the vicinity of ocean boundaries, but limited in the ocean interior relative to the pressure gradient (Tomczak and Godfrey, 2001). The balance between Coriolis force as a result of the rotation of the earth and pressure gradient force is known as the geostrophic flow. In a fluid dominated by rotation, the flow is called geostrophic and is perpendicular to the pressure gradient force encircling centers of low and high pressure as a result of the Coriolis effect (Tally et al., 2011). Figure 4.6 (a)-(c) illustrates the geostrophic flow along the Crossroad transect. The geostrophic flow of the jet is more intense inshore at approximately 36°S and further offshore at approximately 38°S for different years (from 2013 to 2015). The direction of the flow of the AC is negative (south) while the direction of the ARC is positive (east) as expected and corroborated by the altimetry data in Figure 4.1 (a)-(c).

In Figure 4.8 a notable similarity between the AC and ARC is the distribution of the types of water masses at all layers (surface to deep layers) with the exception of intermediate layers. The CTD and TSG measurements in Figure 4.9 are obtained from an iso-surface within a depth range of between 4 and 8 m. A comparison of SSS using CTD and TSG data shows variability along the Crossroad transect. The main purpose of Figure 4.9 is to document the data missing when sampling using CTD instruments. Accuracy of the data collected from CTDs is not provided by the resolution of the CTD, but by the CTD measurements when calibrated. Inconsistency and inacuracy of these measurements is based mainly on the interpretation during data analysis. The same occurs with TSG data. There is a need for finer scale resolution data such as TSG. This allows analysis of small scale features along the Crossroad transect and allow accurate and concrete examination of ocean circulation conditions and processes. The importance of the study is to indicate that small scale features are ubiquitous and knowledge of this features is important for understanding the Agulhas system.

The interannual differences observed along the Crossroad transect are also documented in Figure 4.10 (a)-(c). These differences suggest an influence of eddy features on the water mass properties. This means that the sea surface temperature is expected to be lower in the absence of warm anticyclonic eddies along the AP and thus the presence of eddies have an influence on water properties such as temperature and salinity (Figures 4.11 and 4.12) along the transect. What is novel and appreciative, however is the extent of the variability observed interannually in both the hydrogaphic, current and altimetry datasets. This study resolves well how each dataset potentially gives more detail about the other datasets, providing a more comprehensive view of the ocean dynamics governing the ACS and suggesting a link and a complementary relationship between different datasets. The results overall confirm the predominant structure of the ACS including the dynamics associated with its sources and mesoscale features observed along the Crossroad transect. This was done by analyzing different datasets that highlight an overview of the ACS with scales and resolutions. The study has

therefore explored different basin scale features using different observation tools and most importantly how these components are distinct from time to time. The study has also addressed the minor limitations associated with some of these datasets.

Chapter 6

Conclusion

The overarching aim of the thesis was to understand the variability across the Crossroad transect by answering the following key questions:

1. What basin scale circulation features do we observe across the Crossroad transect?

2. How do observations of basin scale and mesoscale features differ when using different datasets?

3. Are there interannual similarities and differences in the basin scale and mesoscale features observed along the Crossroad transect between 2013 and 2015?

In an attempt to gain a better perspective about the variability across the Crossroad transect, the study brings together the altimetry data from AVISO along with the in situ observations from different products. The coupling of these products highlighted important ocean dynamics across the Crossroad transect. Perharps most important, the spatial and temporal variation within the system. The study outlines the importance of understanding the decisive role played by basin scale and mesoscale features on a local, regional and global context. These include their spatio-temporal variant nature and impact on the ocean circulation. Despite the limitations, this study provides more insight on the regional importance of the Agulhas Current and its return flow. Considering different scales, our planet´s climate is also subject to changes in response to natural variability, hence the need to bring different observation tools to get a clear perspective of how the world will potentially be impacted (Wu et al., 2013). Previous studies have also shown a link between the large scale climate modes such as the Indian Ocean Dipole and El Niño Southern Oscillation (ENSO) with variability in the southwest Indian Ocean (Schouten et al., 2002; de Ruijter et al., 2005). With that being said, climate change has a potential of intensifying the hydrological cycle, which further affects the atmospheric water vapor concentrations, stream flow patterns and precipitation patterns leading to the intensification of drought and floods (Allen and Ingram, 2002). Reason et al., (2006) similarly contend that southern Africa is susceptible to these pronounced floods,

droughts and climate variability at different timescales. This has a potential impact also on the capacity of individuals, communities, institutions, businesses and systems to adapt to such perturbations. Consequently, these climate change factors have a great impact on society (Köhler, 2015). Sweijd et al., (2015) explained the variability of climate dynamics in terms of frequency and intensity and, as a result of drought, local regions such as Western Cape are affected by water shortages where major water reserves are being severely depleted. Considerable variability is also evident through continual observations (though limited) along the Agulhas Current system (Hermes et al., 2007) on both spatial and temporal scales and constant monitoring in this region is necessary.

Although progress has been achieved in the last two decades in characterizing and analyzing different ocean fields using both altimetry and in situ data, our understanding of mesoscale and submesoscale dynamics remains incomplete. Furthermore, the associated practical problem of both understanding and predicting eddy fluxes of heat and other material properties remain unsolved (Klein et al., 2015). The need for repeated global observations at finer spatial and temporal scales is essential. The variable, dynamic and complex circulation associated with the ACS continues to provide a natural laboratory for exploring the potential and limitations of both satellite and in situ observations. The study has therefore managed to improve the characterization of both basin scale and mesoscale variability by examining the dynamics that govern variability across the Crossroad transect. This was done by considering salient features of the Agulhas system, including the Agulhas Current and dynamics associated with its sources. The patterns of this system needs careful attention and continuous monitoring.

The Crossroad transect as the name suggests, forms a cross road as it passes through the Agulhas Current and Agulhas Return Current. For this reason the Agulhas Retroflection and leakage do not form part of the monitoring route and were not considered as part of the data analysis. Although they do not form part of the route, understanding their contribution to the overall ocean circulation has been highlighted through altimetry data. Their role on the Agulhas system has also been investigated (Beal et al., 2011). In addition this study focused on the flow regime of the Agulhas Current as it forms an integrating system through the inter ocean exchange between the Atlantic and Indian Ocean (Boebel et al., 2003) and principal pathways of water mass exchange within the wide basin scale (Benny et al., 2015). This study has provided knowledge on the variability along the Crossroad transect by comparing different datasets, although extensive uncertainties and contradictions were identified (Rouault et al., 2009; Van Sebille et al., 2009). This includes defining both mesoscale leading to submesoscale features and their importance and contribution towards the ocean circulation.

The findings of this study include the altimetry and in situ datasets that are comparable in terms of highlighting variability along the Crossroad transect. Lutjeharms, (2006) highlighted the complex ocean conditions associated with the Agulhas Current system and this study confirms the ocean dynamics related to the Crossroad transect.

Equally important to note is the good correspondence observed between the altimetry and SADCP data, which suggests that in future a synergy of different datasets is beneficial for the comprehension of complex ocean systems and recommended for studies both related and unrelated to physical oceanography. The different datasets used in this study produced different results, resolving both large scale, mesoscale and submesoscale features. This may be due to the different resolutions that are able to capture the submesoscale variability, while others could not. The TSG data however was able to resolve well the submesoscale features. This also shows that it is imoprtant to understand different spatial and temporal resolutions in defining ocean variability along the Crossroad transect.

Evidence shows that the region along which the Crossroad transect exists is subject to a large number of mesoscale and submesoscale features dominated by shear boundary processes such as meanders, eddies and break away filaments (Lutjeharms et al., 1981), which differ on a spatial and temporal scale. The measurements obtained from SADCP data are well resolved and demonstrate the expected fast flowing western boundary current (Lutjeharms, 2001); the AC with velocity measurements of down to 2.4 m/s. Altogether, the careful considerarion of in situ and satellite data suggest that the Crossroad transect is dominated by transient basin scale, mesoscale and submesoscale features. In an attempt to understand the variability across the Crossroad transect using hydrographic data, the study also considered the basin scale circulation, how observations differ when using different datasets and an interannual outlook on both similarities and differences of these features was analyzed. The predominant basin scale features observed along the transect include the Agulhas Current and Agulhas Return Current.

An implicit limitation of the study lies in the low resolution CTD data that is unable to resolve well some of the submesoscale features due to limited spatial coverage. The aim of the study was to show that sufficient data is uncaptured and often overlooked when using low resolution CTD data. Comparing the high resolution TSG dataset with CTD data, innumerable submesoscale features including fronts and filaments are identified, making TSG data more efficient in resolving small scale features along the Crossroad transect. The fronts identified are also known to have an influence on the biomass of phytoplankton by introducing nutrients from different water masses (Swart et al., 2012). Therefore, a recommendation would be to intentionally focus on the submesoscale features as these small scale features also contribute to the overall global ocean circulation. In addition, data collection for the Crossroad transect takes place annually (April-May) through the Marion Island voyage, therefore oceanographic observations are not enough as no seasonal record is provided.

Although the study has dealt with the initialization of a valuable and broader investigation into the variability in basin scale and mesoscale features across the Crossroad transect, more work still needs to be done to fill in the uncertainties in this region. In addition, it is worth noting that the water masses associated with the AC should be well

understood as they play a crucial role in influencing the primary productivity that occurs along the Agulhas Bank. The cold nutrient-rich SICW upwelled onto the shelf play an important role in the spawning of various fish species such as Cape Anchovy (Van der Lingen et al., 2001). Therefore, the effect of the AC not only on the shelf, but also throughout the vertical water column south of Africa must be monitored. Spatial and temporal processes relating to the Agulhas system have been highlighted to demonstrate the importance of this system for the future scientific community.

6.1 Future Research

The role played by eddies across the basin scale is important. Further research on their properties is essential including their lifespan and retention time, translation speed (trajectory), eddy scale (size or dimension), eddy rotational speeds and eddy vertical structure. These can be conducted through satellite derived altimetry data and high resolution model simulations using an eddy automated detection scheme (Collins et al., 2014). It is worth noting that the procedure for an eddy detecting scheme requires a longer time series and the Crossroad transect data used in this research consists of three years of data, which is already noted as one of the limitations of the study. However, for future research once this region has enough seasonal datasets, consideration for eddy detecting is highly recommended. Thus, the need for advancement and development of ocean observations is necessary including collaborations of different ocean disciplines. It is therefore advisable for potential academics across South Africa and globally to unite and investigate measures that will fill the continual spatio-temporal gaps (Collins et al., 2014). In addition, although countless challenges are inevitable in the ocean science community, these advances are further required in public awareness campaigns of the ocean environment and climate (Dickey, 2003). Formulation, accuracy and efficiency of data assimilative ocean models are required across the Crossroad transect for the validation of interdisciplinary observational data (Dickey, 2003; Hermes et al., 2006). Incorporation of ocean models such as Regional Ocean Model System (ROMS) in this study is also recommended.

Seasonal variability is necessary to improve current knowledge on the Agulhas system given that the study focused on the spatio-temporal variability of both basin and mesoscale features. The inclusion of Lagrangian methods is important as they provide solutions to the challenges, which have a major impact on risk management processes such as control of pollution dispersion (Hernández-Carrasco et al., 2011). Additionally, they also provide sufficient information on ecosystem analysis that include, but not limited to tracking nutrient mixing and transport and identifying the role of horizontal mixing in primary productivity. Altogether these Lagrangian techniques advance necessary information about the energy exchanges that influence the upper ocean and will assist in the full comprehension of processes that drive the global change in the oceans

(Hernández-Carrasco et al., 2011). An investment in sufficient computational resources promises a better assessment tool of the transport role played by mesoscale eddies in the local, regional and global ocean circulation and climate (Beron-Vera et al., 2013). There is no evidence of high resolution glider data to infer on the biogeochemical measurements that influence the mesoscale and submesoscale features along the Crossroad transect and this essentially remains one of the limitations of the study as mentioned in Chapter 1. A complete understanding of the behaviour of the basin scale, mesoscale and submesoscale dynamics requires as well more comprehensive observing systems, the kind that extends across neighboring ocean basins. Such a system may include not only Argo floats, gliders and satellite data that are limited to the upper ocean, but also moored instruments that encompass the full depth ocean column (Ansorge et al., 2014). Therefore, this study also recommends the inclusion of gliders and Argo floats along the Crossroad transect to fully understand the volume transport, water mass exchange and other oceanographic conditions that are associated with the Agulhas Current system.

Model experiments with advanced forcing and observational evidence over a wider time frame and a wider domain are also necessary for the comprehension of the ocean circulation across the Crossroad transect. In addition, an integration of both model, altimetry and in situ datasets will assist in playing an integral role towards a quantitative understanding the ocean atmosphere interactions and ocean circulation affecting the thermohaline circulation (Backeberg, 2009). It is interesting to note that the anticyclonic eddies observed along the transect indicate slightly different surface water properties relative to the surrounding waters thus having an influence on the density in the region (Maes et al., 2014). In addition, eddies also play a potential vector role in transporting planktonic larvae and water masses (Braby, 2014). Furthermore, understanding the ocean circulation around the Crossroad transect is essential and will benefit future studies that monitor both the Atlantic and Indian Ocean and other potential projects that monitor routes such as the South Atlantic MOC Basin wide Array (SAMBA), Agulhas System Climate Array (ASCA) and GoodHope line. Although the Agulhas Current and Agulhas Return Current do not intersect the aforementioned monitoring lines (SAMBA and GoodHope line), mesoscale features occluded from these currents have an influence on the water properties associated with these transects (Faure et al., 2011).

Future research should therefore aim to explore the interactions, dynamics and ecosystem implications that are established by both mesoscale and submesoscale features across the Crossroad transect. An understanding of the interstitial or frontal flow between eddies is also required. Although more work still needs to be done, this study has shown the importance of understanding the nature of processes that are affected by both temporal and spatial scales and how they differ using different observing systems as summarized in Figure 2.1. To recapitulate, in view of the impact that small scale features have on the ocean circulation across the Crossroad transect, as also suggested by recent ocean model studies (Halo et al., 2014, Backeberg et al., 2012; Weijer et al, 2002), it seems

consequential to advance studies of the nature of complex connections with large scale ocean circulation brought about by eddies south of Africa. Therefore, using 3 years of hydrographic data across the Crossroad transect, has led to an appreciation of the variability in this study region and more curiosity of the diverse knowledge that is yet to be discovered.

Bibliography

Ansorge, I. J., Baringer, M. O., Campos, E. J., Dong, S., Fine, R. A., Garzoli, S. L., ... & Roberts, M. J. (2014). BasinWide Oceanographic Array Bridges the South Atlantic. Eos, Transactions American Geophysical Union, 95(6), 53-54.

Ansorge, I. J., (2013). South African National Antarctic Programme (SANAP) voyage participation Report, 1-15.

Ansorge, I. J., (1996). The structure and transport of the Agulhas Return Current. (Masters, University of Cape Town), 9

Artale, V., Boffetta, G., Celani, A., Cencini, M., & Vulpiani, A. (1997). Dispersion of passive tracers in closed basins: Beyond the diffusion coefficient. Physics of Fluids, 9(11), 3162-3171.

Aslebagh, S. (2013). Development Of An Oceanic Rain Accumulation Product In Support Of Sea Surface Salinity Measurements From Aquarius/sac-d (Doctoral dissertation, University of Central Florida Orlando, Florida).

Backeberg, B. C., Counillon, F., Johannessen, J. A., & Pujol, M. I. (2014). Assimilating along-track SLA data using the EnOI in an eddy resolving model of the Agulhas system. Ocean Dynamics, 64(8), 1121-1136.

Backeberg, B. C., Penven, P., & Rouault, M. (2012). Impact of intensified Indian Ocean winds on mesoscale variability in the Agulhas system. Nature Climate Change, 2(8), 608-612.

Beal, L. M., De Ruijter, W. P., Biastoch, A., & Zahn, R. (2011). On the role of the Agulhas system in ocean circulation and climate. Nature, 472(7344), 429-436.

Beal, L., & Biastoch, A. (2010). Improving Understanding of the Agulhas Current and Its Global Climate Impacts: Working Group on the Climatic Importance of the Greater Agulhas System; Portland, Oregon, 2021 February 2010. Eos, Transactions American Geophysical Union, 91(18), 163-163.

Beal, L. M., Chereskin, T. K., Lenn, Y. D., & Elipot, S. (2006). The sources and mixing characteristics of the Agulhas Current. Journal of physical oceanography, 36(11), 2060-2074.

Beal, L. M., & Bryden, H. L. (1997). Observations of an Agulhas undercurrent. Deep Sea Research Part I: Oceanographic Research Papers, 44(9), 1715-1724.

Belkin, I. M., & Gordon, A. L. (1996). Southern Ocean fronts from the Greenwich meridian to Tasmania. Journal of Geophysical Research: Oceans, 101(C2), 3675-3696.

Benny, N. P., Shenbakavalli, R., Mazlan, H., Mohd, N. R., & Mohd, R. M. (2015). Mesoscale surface circulation and variability of Southern Indian Ocean derived by combining satellite altimetry and drifter observations. Acta Oceanologica Sinica, 34(9), 12-22.

Beron-Vera, F. J., Wang, Y., Olascoaga, M. J., Goni, G. J., & Haller, G. (2013). Objective detection of oceanic eddies and the Agulhas leakage. Journal of Physical Oceanography, 43(7), 1426-1438.

Biastoch, A., Böning, C. W., Schwarzkopf, F. U., & Lutjeharms, J. R. E. (2009). Increase in Agulhas leakage due to poleward shift of Southern Hemisphere westerlies. Nature, 462(7272), 495-498.

Biastoch, A., Lutjeharms, J. R. E., Böning, C. W., & Scheinert, M. (2008). Mesoscale perturbations control interocean exchange south of Africa. Geophysical Research Letters, 35(20).

Biastoch, A., & Krauss, W. (1999). The role of mesoscale eddies in the source regions of the Agulhas Current. Journal of Physical Oceanography, 29(9), 2303-2317.

Boebel, O., Rossby, T., Lutjeharms, J., Zenk, W., & Barron, C. (2003). Path and variability of the Agulhas Return Current. Deep Sea Research Part II: Topical Studies in Oceanography, 50(1), 35-56.

Boutin, J., Chao, Y., Asher, W. E., Delcroix, T., Drucker, R., Drushka, K., ... & Schanze, J. (2015). Satellite and in situ salinity: Understanding near-surface stratification and sub-footprint variability. Bulletin of the American Meteorological Society.

Braby, L. (2014). Dynamics, interactions and ecosystem implications of mesoscale eddies formed in the southern region of Madagascar (Master of Science dissertation, University of Cape Town).

Bryden, H. L., & Beal, L. M. (2001). Role of the Agulhas Current in Indian Ocean circulation and associated heat and freshwater fluxes. Deep Sea Research Part I: Oceanographic Research Papers, 48(8), 1821-1845.

Bryden, H. L., Beal, L. M., & Duncan, L. M. (2005). Structure and transport of the Agulhas Current and its temporal variability. Journal of Oceanography, 61(3), 479-492.

Chavanne, C. P., & Klein, P. (2010). Can oceanic submesoscale processes be observed with satellite altimetry?. Geophysical Research Letters, 37(22).

Chelton, D. B., Schlax, M. G., & Samelson, R. M. (2011). Global observations of nonlinear mesoscale eddies. Progress in Oceanography, 91(2), 167-216.

Collins, C., Hermes, J. C., & Reason, C. J. C. (2014). Mesoscale activity in the Comoros Basin from satellite altimetry and a highresolution ocean circulation model. Journal of Geophysical Research: Oceans, 119(8), 4745-4760.

Cooper, K. F. (2014). Evaluating global ocean reanalysis systems for the greater Agulhas Current System.(Master of Science, dissertation, University of Cape Town).

Cunningham, S. A., Kanzow, T., Rayner, D., Baringer, M. O., Johns, W. E., Marotzke, J., ... & Meinen, C. S. (2007). Temporal variability of the Atlantic meridional overturning circulation at 26.5 N. Science, 317(5840), 935-938.

Daniault, N., & Ménard, Y. (1985). Eddy kinetic energy distribution in the Southern Ocean from altimetry and FGGE drifting buoys. Journal of Geophysical Research: Oceans, 90(C6), 11877-11889.

Darbyshire, J. (1972). The effect of bottom topography on the Agulhas Current. Pure and Applied Geophysics, 101(1), 208-220.

Dencausse, G., Arhan, M., & Speich, S. (2010). Spatio-temporal characteristics of the Agulhas Current retroflection. Deep Sea Research Part I: Oceanographic Research Papers, 57(11), 1392-1405.

de Ruijter, W. P., van Aken, H. M., Beier, E. J., Lutjeharms, J. R., Matano, R. P., & Schouten, M. W. (2004). Eddies and dipoles around South Madagascar: formation, pathways and large-scale impact. Deep Sea Research Part I: Oceanographic Research Papers, 51(3), 383-400.

de Ruijter, W. P., Ridderinkhof, H., Lutjeharms, J. R., Schouten, M. W., & Veth, C. (2002). Observations of the flow in the Mozambique Channel. Geophysical Research Letters, 29(10).

de Ruijter, W. (1982). Asymptotic analysis of the Agulhas and Brazil Current systems. Journal of Physical Oceanography, 12(4), 361-373.

Dong, C., McWilliams, J. C., Liu, Y., & Chen, D. (2014). Global heat and salt transports by eddy movement. Nature Communications, 5.

Ducet, N., Le Traon, P. Y., & Reverdin, G. (2000). Global highresolution mapping of ocean circulation from TOPEX/Poseidon and ERS1 and2. Journal of Geophysical Research: Oceans, 105(C8), 19477-19498.

Durack, P. J., Wijffels, S. E., & Matear, R. J. (2012). Ocean salinities reveal strong global water cycle intensification during 1950 to 2000. science, 336(6080), 455-458.

Durand, F., Alory, G., Dussin, R., & Reul, N. (2013). SMOS reveals the signature of Indian Ocean Dipole events. Ocean Dynamics, 63(11-12), 1203-1212.

Emery, W. J. (2001). Water types and water masses. Encyclopedia of Ocean Sciences, 6, 3179-3187.

Faure, V., Arhan, M., Speich, S., & Gladyshev, S. (2011). Heat budget of the surface mixed layer south of Africa. Ocean Dynamics, 61(10), 1441-1458.

Ferrari, R., & Wunsch, C. (2009). Ocean circulation kinetic energy: Reservoirs, sources, and sinks. Annual Review of Fluid Mechanics, 41, 253-282.

Gamoyo, M., Reason, C. J., & Collins, C. (2017). A numerical investigation of the Southern Gyre using ROMS. Journal of Marine Systems.

Gaultier, L., Verron, J., Brankart, J. M., Titaud, O., & Brasseur, P. (2013). On the inversion of submesoscale tracer fields to estimate the surface ocean circulation. Journal of Marine Systems, 126, 33-42.

Gille, S. T. (2003). Float observations of the Southern Ocean. Part I: Estimating mean fields, bottom velocities, and topographic steering. Journal of Physical Oceanography, 33(6), 1167-1181.

Gordon, A. L., Weiss, R. F., Smethie, W. M., & Warner, M. J. (1992). Thermocline and intermediate water communication between the South Atlantic and Indian Oceans. Journal of Geophysical Research: Oceans, 97(C5), 7223-7240.

Gordon, A. L. (1985). Indian-Atlantic transfer of thermocline water at the Agulhas Retroflection. Science, 227(4690), 1030-1033.

Gründlingh, M. L. (1983). On the course of the Agulhas Current. South African Geographical Journal, 65(1), 49-57.

Gründlingh, M. L. (1978). Drift of a satellite-tracked buoy in the southern Agulhas Current and Agulhas Return Current. Deep Sea Research, 25(12), 1209-1224.

Hall, C., & Lutjeharms, J. R. E. (2011). Cyclonic eddies identified in the Cape Basin of the South Atlantic Ocean. Journal of Marine Systems, 85 (1), 1-10.

Halo, I., Backeberg, B., Penven, P., Ansorge, I., Reason, C., & Ullgren, J. E. (2014). Eddy properties in the Mozambique Channel: A comparison between observations and two numerical ocean circulation models. Deep Sea Research Part II: Topical Studies in Oceanography, 100, 38-53.

Halo, I. F.M (2012). The Mozambique Channel Eddies: Characteristics and mechanisms of formation, University of Cape Town (Doctor of Philosophy, University of Cape Town), 1-231.

Hermes, J. C., Reason, C. J. C., & Lutjeharms, J. R. E. (2007). Modeling the variability of the greater Agulhas Current system. Journal of Climate, 20(13), 3131-3146.

Hernández-Carrasco, I., López, C., Hernández-García, E., & Turiel, A. (2011). How reliable are finite-size Lyapunov exponents for the assessment of ocean dynamics?. Ocean Modelling, 36(3), 208-218.

Hofmann, E. E. (1985). The largescale horizontal structure of the Antarctic Circumpolar Current from FGGE drifters. Journal of Geophysical Research: Oceans, 90(C4), 7087-7097.

Hutchings, L., Beckley, L. E., Griffiths, M. H., Roberts, M. J., Sundby, S., & Van der Lingen, C. (2002). Spawning on the edge: spawning grounds and nursery areas around the southern African coastline. Marine and Freshwater Research, 53(2), 307-318.

Imawaki, S., Bower, A. S., Beal, L., Qui, B. (2013) Western Boundary Currents, Ocean Circulation and Climate, Vol. 103, 305-338.

Jury, M., & Walker, N. (1988). Marine boundary layer modification across the edge of the Agulhas Current. Journal of Geophysical Research: Oceans, 93(C1), 647-654.

Kolodziejczyk, N., Reverdin, G., Boutin, J., & Hernandez, O. (2015). Observation of the surface horizontal thermohaline variability at mesoscale to submesoscale in the northeastern subtropical Atlantic Ocean. Journal of Geophysical Research: Oceans, 120 (4), 2588-2600.

Köhler, Julia. "Sea Surface Salinity Variability and Underlying Mechanisms: an analysis and interpretation of satellite data." (2015).

Kuhlbrodt, T., Griesel, A., Montoya, M., Levermann, A., Hofmann, M., & Rahmstorf, S. (2007). On the driving processes of the Atlantic meridional overturning circulation. Reviews of Geophysics, 45(2).

Largier, J. L., Chapman, P., Peterson, W. T., & Swart, V. P. (1992). The western Agulhas Bank: circulation, stratification and ecology. South African Journal of Marine Science, 12(1), 319-339.

Lamont, T., Barlow, R. G., Morris, T., & Van Den Berg, M. A. (2014). Characterization of mesoscale features and phytoplankton variability in the Mozambique Channel. Deep Sea Research Part II: Topical Studies in Oceanography, 100, 94-105.

Loveday, B. (2014). Modelling wind-driven inter-ocean exchange in the greater Agulhas with the Regional Ocean Modelling System (Doctoral dissertation, University of Cape Town).

L'Ecuyer, T. S., Beaudoing, H. K., Rodell, M., Olson, W., Lin, B., Kato, S., ... & Huffman, G. (2015). The observed state of the energy budget in the early twenty-first century. Journal of Climate, 28(21), 8319-8346.

Lévy, M., Ferrari, R., Franks, P. J., Martin, A. P., & Rivire, P. (2012). Bringing physics to life at the submesoscale. Geophysical Research Letters, 39(14).

*L'*Hégaret, P., Carton, X., Louazel, S., & Boutin, G. (2015). Mesoscale eddies and submesoscale structures of Persian Gulf Water off the Omani coast in Spring 2011. Ocean Science Discussions, 12(6).

Lutjeharms, J. R. (2006). The agulhas current (p. 330). Berlin: Springer.

Lutjeharms, J. R. E., & Ansorge, I. J. (2001). The Agulhas return current. Journal of Marine Systems, 30(1), 115-138.

Lutjeharms, J. R. E., & Cooper, J. (1996). Interbasin leakage through Agulhas Current filaments. Deep Sea Research Part I: Oceanographic Research Papers, 43(2), 213-238.

Lutjeharms, J. R. E., & De Ruijter, W. P. M. (1996). The influence of the Agulhas Current on the adjacent coastal ocean: possible impacts of climate change. Journal of Marine Systems, 7(2), 321-336.

Lutjeharms, J. R. E., Bang, N. D., & Duncan, C. P. (1981). Characteristics of the currents east and south of Madagascar. Deep Sea Research Part A. Oceanographic Research Papers, 28(9), 879-899.

Lutjeharms, J. R. E., & Van Ballegooyen, R. C. (1984). Topographic control in the Agulhas Current system. Deep Sea Research Part A. Oceanographic Research Papers, 31(11), 1321-1337.

Lutjeharms, J. R. E., & Van Ballegooyen, R. C. (1988). The retroflection of the Agulhas Current. Journal of Physical Oceanography, 18(11), 1570-1583.

Maes, C., Dewitte, B., Sudre, J., Garon, V., & Varillon, D. (2013). Smallscale features of temperature and salinity surface fields in the Coral Sea. Journal of Geophysical Research: Oceans, 118(10), 5426-5438.

Maes, C., Reul, N., Behringer, D., & OKane, T. (2014). The salinity signature of the equatorial Pacific cold as revealed by the satellite SMOS mission. GeoScience Letters, 1(1), 1.

McPhaden, M. J., & Zhang, D. (2002). Slowdown of the meridional overturning circulation in the upper Pacific Ocean. Nature, 415(6872), 603-608.

McWilliams, J. C. (2016, May). Submesoscale currents in the ocean. In Proc. R. Soc. A (Vol. 472, No. 2189, p. 20160117). The Royal Society.

Melato, L. I. (2012). The role of Mesoscale Eddies on the Carbon Dioxide Flux in the Antarctic Polar Frontal Zone of the South-West Indian Ocean

Meredith, M. P., & Hogg, A. M. (2006). Circumpolar response of Southern Ocean eddy activity to a change in the Southern Annular Mode. Geophysical Research Letters, 33(16).

Morris, T., Hermes, J., Beal, L., du Plessis, M., Rae, C. D., Gulekana, M., ... & Ansorge, I. J. (2017). The importance of monitoring the Greater Agulhas Current and its inter-ocean exchanges using large mooring arrays. South African Journal of Science, 113(7-8), 1-7.

Morris, T., Lamont, T., & Roberts, M. J. (2013). Effects of deep-sea eddies on the northern KwaZulu-Natal shelf, South Africa. African Journal of Marine Science, 35(3), 343-350.

Morisset, S., Reverdin, G., Boutin, J., Martin, N., Yin, X., Gaillard, F., ... & Salvador, J. (2012). Surface salinity drifters for SMOS validation. Mercator OceanCORIOLIS Quarterly Newsletter, (45), 33-37.

Nyadjro, E. S., & Subrahmanyam, B. (2016). Spatial and temporal variability of central Indian Ocean salinity fronts observed by SMOS. Remote Sensing of Environment, 180, 146-153.

Peeters, F. J., Acheson, R., Brummer, G. J. A., De Ruijter, W. P., Schneider, R. R., Ganssen, G. M., ... & Kroon, D. (2004). Vigorous exchange between the Indian and Atlantic oceans at the end of the past five glacial periods. Nature, 430(7000), 661-665.

Quartly, G. D., & Srokosz, M. A. (2004). Eddies in the southern Mozambique Channel. Deep Sea Research Part II: Topical Studies in Oceanography, 51(1), 69-83.

Richardson, P. L. (1983). Eddy kinetic energy in the North Atlantic from surface drifters. Journal of Geophysical Research: Oceans, 88(C7), 4355-4367.

Ridgway, K. R., & Dunn, J. R. (2003). Mesoscale structure of the mean East Australian Current System and its relationship with topography. Progress in Oceanography, 56(2), 189-222.

Ridderinkhof, H., Van der Werf, P. M., Ullgren, J. E., Van Aken, H. M., Van Leeuwen, P. J., & De Ruijter, W. P. M. (2010). Seasonal and interannual variability in the Mozambique Channel from moored current observations. Journal of Geophysical Research: Oceans, 115(C6).

Rio, M. H., & Hernandez, F. (2004). A mean dynamic topography computed over the world ocean from altimetry, in situ measurements, and a geoid model. Journal of Geophysical Research: Oceans, 109(C12).

Roberts, M. J. (2005). Chokka squid (Loligo vulgaris reynaudii) abundance linked to changes in South Africa's Agulhas Bank ecosystem during spawning and the early life cycle. ICES Journal of Marine Science: Journal du Conseil, 62(1), 33-55.

Robinson, A. R. (1983). Overview and summary of eddy science. In Eddies in marine science (pp. 3-15). Springer Berlin Heidelberg.

Rouault, M. J., & Penven, P. (2011). New perspectives on Natal Pulses from satellite observations. Journal of Geophysical Research: Oceans, 116(C7).

Rouault, M., Penven, P., & Pohl, B. (2009). Warming in the Agulhas Current system since the 1980's. Geophysical Research Letters, 36(12).

Rouault, M., Reason, C. J. C., Lutjeharms, J. R. E., & Beljaars, A. C. M. (2003). Underestimation of latent and sensible heat fluxes above the Agulhas Current in NCEP and ECMWF analyses. Journal of Climate, 16(4), 776-782.

Ruijter, W. D., Biastoch, A., Drijfhout, S. S., Lutjeharms, J. R. E., Matano, R. P., Pichevin, T., ... & Weijer, W. (1999). IndianAtlantic interocean exchange: Dynamics, estimation and impact. Journal of Geophysical Research: Oceans, 104(C9), 20885-20910.

Sabine, C. L., Feely, R. A., Gruber, N., Key, R. M., Lee, K., Bullister, J. L., ... & Millero, F. J. (2004). The oceanic sink for anthropogenic CO2. Science, 305(5682), 367-371.

Schiermeier, Q. (2007). Climate change 2007: What we don't know about climate change. Nature, 445(7128), 580-581.

Schiermeier, Q. (2013). Oceans under surveillance. Nature, 497(7448), 167-168.

Schiermeier, Q. (2007). Climate change 2007: What we don't know about climate change. Nature, 445(7128), 580-581.

Schmittner, A., Chiang, J. C., & Hemming, S. R. (2007). Introduction: The ocean's meridional overturning circulation. Ocean Circulation: Mechanisms and Impacts-Past and Future Changes of Meridional Overturning, 1-4.

Schott, F. A., & McCreary Jr, J. P. (2001). The monsoon circulation of the Indian Ocean. Progress in Oceanography, 51(1), 1-123.

Schouten, M. W., de Ruijter, W. P., & van Leeuwen, P. J. (2002). Upstream control of Agulhas Ring shedding. Journal of Geophysical Research: Oceans, 107(C8).

Shillington, F. A., Reason, C. J. C., Rae, C. D., Florenchie, P., & Penven, P. (2006). 4 Large scale physical variability of the Benguela Current Large Marine Ecosystem (BCLME). Large marine ecosystems, 14, 49-70.

Siedler, G., Rouault, M., Biastoch, A., Backeberg, B., Reason, C. J., & Lutjeharms, J. R. (2009). Modes of the southern extension of the East Madagascar Current. Journal of Geophysical Research: Oceans, 114(C1).

Stephens, G. L., Li, J., Wild, M., Clayson, C. A., Loeb, N., Kato, S., ... & Andrews, T. (2012). An update on Earth's energy balance in light of the latest global observations. Nature Geoscience, 5(10), 691-696.

Stramma, L., & Lutjeharms, J. R. (1997). The flow field of the subtropical gyre of the South Indian Ocean. Journal of Geophysical Research: Oceans, 102(C3), 5513-5530.

Swart, S., Thomalla, S. J., Monteiro, P. M. S., & Ansorge, I. J. (2012). Mesoscale features and phytoplankton biomass at the GoodHope line in the Southern Ocean during austral summer. African Journal of Marine Science, 34(4), 511-524.

Sweijd, N. A., Wright, C. Y., Westwood, A., Rouault, M., Landman, W. A., MacKenzie, M. L., ... & Berhoozi, F. (2015). Climate change is catchy-but when will it really hurt?. SAMJ: South African Medical Journal, 105(12), 1018-1023.

Talley, L. D. (2011). Descriptive physical oceanography: an introduction. Academic press.

Tandeo, P., Chapron, B., Ba, S., Autret, E., & Fablet, R. (2014). Segmentation of mesoscale ocean surface dynamics using satellite SST and SSH observations. IEEE Transactions on Geoscience and Remote Sensing, 52(7), 4227-4235.

Toggweiler, J. R., Russell, J. L., & Carson, S. R. (2006). Midlatitude westerlies, atmospheric CO2, and climate change during the ice ages. Paleoceanography, 21(2).

Tomczak, M., & Godfrey, J. S. (2013). Regional oceanography: an introduction. Elsevier.

Toole, J. M., & McDougall, T. J. (2001). 2 Mixing and stirring in the ocean interior. International Geophysics, 77, 337-355.

Trenberth, K. E., Fasullo, J. T., & Kiehl, J. (2009). Earth's global energy budget. Bulletin of the American Meteorological Society, 90(3), 311.

Van den Berg (2015) SANAP 3 2015 (DEA Research) Marion Relief Voyage 2015 of MV SA Agulhas II.

Van der Lingen, C. D., Hutchings, L., Merkle, D., Van der Westhuizen, J. J., & Nelson, J. (2001). Comparative spawning habitats of anchovy (Engraulis capensis) and sardine (Sardinops sagax) in the southern Benguela upwelling ecosystem. Spatial processes and management of marine populations, 185-209.

Van Sebille, E., Barron, C. N., Van Leeuwen, P. J., Vossepoel, F. C., & De Ruijter, W. P. M. (2009). Relating Agulhas leakage to the Agulhas Current retroflection location. Ocean science, 5(4), 511-521.

Watson, A. J., & Naveira Garabato, A. C. (2006). The role of Southern Ocean mixing and upwelling in glacialinterglacial atmospheric CO2 change. Tellus B, 58(1), 73-87.

Wyrtki, Klaus, Lorenz Magaard, and James Hager. "Eddy energy in the oceans." Journal of Geophysical Research 81.15 (1976): 2641-2646.

Yang, H., Lohmann, G., Wei, W., Dima, M., Ionita, M., & Liu, J. (2016). Intensification and poleward shift of subtropical western boundary currents in a warming climate. Journal of Geophysical Research: Oceans, 121(7), 4928-4945.

Yu, L. (2011). A global relationship between the ocean water cycle and nearsurface salinity. Journal of Geophysical Research: Oceans, 116(C10).

Yu, L. (2007). Global variations in oceanic evaporation (1958-2005): The role of the changing wind speed. Journal of Climate, 20(21), 5376-5390.